4 Carbene complexes of Dithienothiophene

1. General

Dithienothiophenes (DTT) are polycondensed heteroaromatic molecules consisting of three condensed thiophene rings. New interest in compounds of this type arose since dithienothiophenes possess three different types of π-conjugation which play an important role as a spacer and donor[1] and these compounds give rise to conjugated polymers with unique properties[2]. The first compound of this series, dithieno[2,3-*b*:3',2'-*d*]thiophene (**II**), was prepared by Pandya and Tilak[3] who cyclized 2,5-bis(dimethoxyethylthio)thiophene with polyphosphoric acid. Altogether six isomers of dithienothiophene are known and have been synthesized (figure 4.1). Although dithieno[3,2-*b*:2',3'-*d*]thiophene (**I**) has been prepared and employed in various syntheses[4], the synthetic inconvenience of dithieno[2,3-*b*:3',2'-*d*]thiophene (**II**) and dithieno[3,4-*b*:3',4'-*d*]thiophene (**III**) had prevented the use of these substrates in organic synthesis in the past. Recently, however, Iyoda *et al*[5] reported a convenient method for the synthesis of **II** and **III** which involves the palladium-catalyzed cyclization of a dibromo-precursor.

Complexes **IV** and **V** were prepared by De Jong *et al*[6] *via* the appropriate dibromo intermediates followed by oxidative ring closure using copper(II) chloride. Compound **VI** was synthesized by converting the suitable dibromodithienyl intermediate into an unstable thiol which, without isolation, was treated with cuprous oxide to yield dithieno[2,3-*b*:2',3'-

---

[1] K. Yui, H. Ishida, Y. Aso, T. Otsubo, F. Ogura, *Chem. Lett.*, **1987**, 2339.

[2] C. Taliani, G. Ruani, R. Zanboni, *Synth. Met.*, 28, **1989**, C507.

[3] L.J. Pandya, B.D. Tilak, *J. Sci. Ind. Res., Sect. B*, 18, **1959**, 371.

[4] F. de Jong, M.J. Janssen, *J. Org. Chem.*, 36, **1971**, 1645.

[5] M. Iyoda, M. Miura, S. Sasaki, S.M.H. Kabir, Y. Kuwatani, M. Yoshida, *Tetrahedron Lett.*, 38, **1997**, 4581.

[6] F. de Jong, M.J. Janssen, *J. Org. Chem.*, 36, **1971**, 1998.

d]thiophene[7]. The relative electrophilic reactivity[8] of compounds **I**, **II** and **VI** were determined by the detritiation of all positions of the isomeric dithienothiophenes in trifluoroacetic acid at 70°C. The results showed that the order of reactivity for the three compounds are **II** > **VI** > **I** for the α-position and **VI** > **II** > **I** for the β-position.

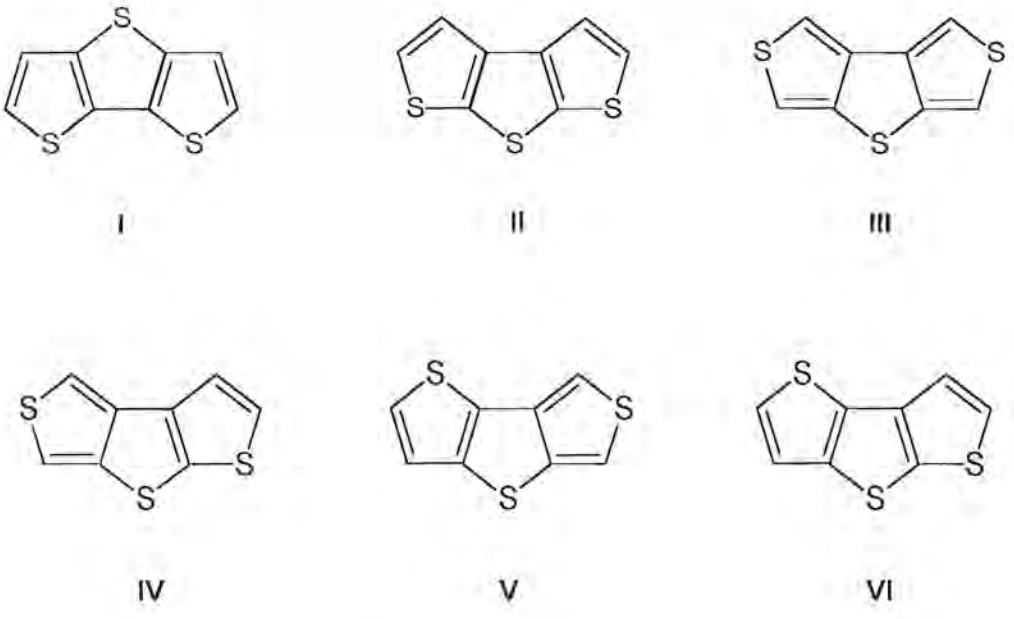

Figure 4.1 Dithienothiophenes

Since a rigid backbone and bulky groups are required in the design of host molecules for crystalline inclusion compounds[9], Mazaki *et al*[10] designed a new host series using linearly condensed thiophenes. They have synthesized a series of compounds (figure 4.2) since the rigid belt-like structure of condensed thiophenes is expected to provide a range of inclusion capacities and cavities in the crystals. The host compounds were prepared by dilithiation of the precursor thiophene derivative followed by treatment with cyclohexylketone, benzophenone and fluorenone. High yields were obtained.

---

[7] K.T. Potts, D. McKeough, *J. Am. Chem. Soc.*, 95, **1973**, 2750.

[8] W.J. Archer, R. Taylor, *J. Chem. Soc., Perkin Trans. 2*, **1982**, 301.

[9] J.L. Atwood, J.E.D. Davies, D.D. MacNicol, *Inclusion Compounds*, Academic Press, London, **1984**.

[10] Y. Mazaki, N. Hayashi, K. Kobayashi, *J. Chem. Soc., Chem. Commun.*, **1992**, 1381.

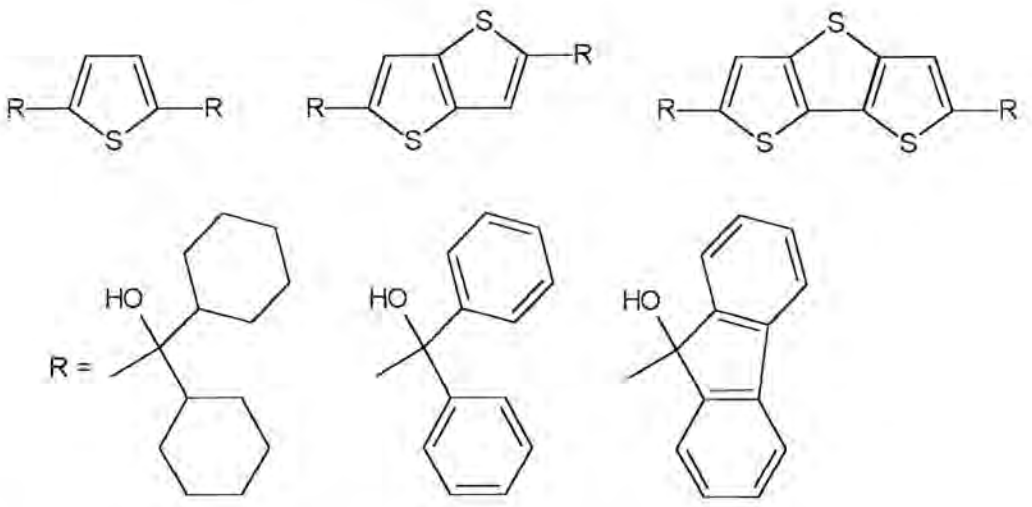

Figure 4.2 Inclusion compounds of thiophene derivatives

Polymerization of compounds **I**, **II** and **III** has received considerable attention lately. Li *et al*[11] reported the design and synthesis of new organic semiconductors for thin film transistors (TFT) application using dithieno[3,2-*b*:2',3'-*d*]thiophene (**I**) as building block. In previous studies it was observed that the dimer of the fused thiophene α,α'-bis(dithieno[3,2-*b*:2',3'-*d*]thiophene) (BDT) was found to have an unusual π-stacked structure and high conducting properties. The synthesis of polymeric dithieno[3,4-*b*:3',4'-*d*]thiophene (**III**) *via* electrochemical polymerization was reported by Catellani *et al*[12].

The coordination properties of dithienothiophene with transition metal complexes have not yet been investigated.

2. Synthesis of Dithieno[3,2-*b*:2',3'-*d*]thiophene

The synthesis of dithieno[3,2-*b*:2',3'-*d*]thiophene (**I**) was based on the work done by De Jong and Janssen[4], where 3-bromothiophene is used as starting material. The general reaction scheme is set out in figure 4.3. The yields of the products, however, could not be met and the oxidative ring closure step (step **c**, figure 4.3), especially proved to be challenging.

---

[11] X. Li, H. Sirringhaus, F. Garnier, A.B. Holmes, S.C. Moratti, N. Feeder, W. Clegg, S.J. Teat, R.H. Friend, *J. Am. Chem. Soc.*, 120, **1998**, 2206.

[12] M. Catellani, T. Caronna, S.V. Meille, *J. Chem. Soc., Chem. Commun.*, **1994**, 1911.

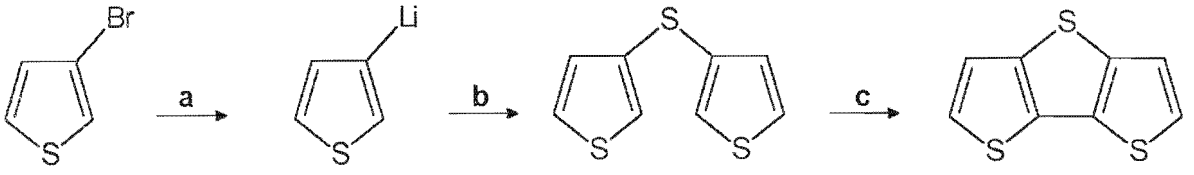

Figure 4.3 Reagents: **(a)** n-BuLi, ether, reflux; **(b)** $(C_6H_5SO_2)_2S$, ether, -70°C; **(c)** 2 n-BuLi, $CuCl_2$

Since this synthesis was time-consuming and the reaction yields were unsatisfactory, a new synthetic route was considered, using 2,2'-bithiophene as starting material. The idea for this synthesis originated from work done by Ohshita *et al*[13]. Dithienosiloles were afforded when 3,3'-dilithio-5,5'-bis(trimethylsilyl)-2,2'-bithiophene, prepared from the reaction of n-butyllithium and 3,3'-dibromo-5,5'-bis(trimethylsilyl)-2,2'-bithiophene, was treated with dichlorodiphenylsilane. Replacement of the silyl groups with bromine atoms yielded dibromodithienosilole. Lithiation and the subsequent hydrolysis of the resulting dilithiodithienosilole afforded 4,4-diphenyldithienosilole. The prospect of utilizing this synthetic method to synthesize dithieno[3,2-*b*:2',3'-*d*]thiophene by substituting dichlorodiphenylsilane for sulfur dichloride was suggested. The proposed reaction scheme is outlined in figure 4.4.

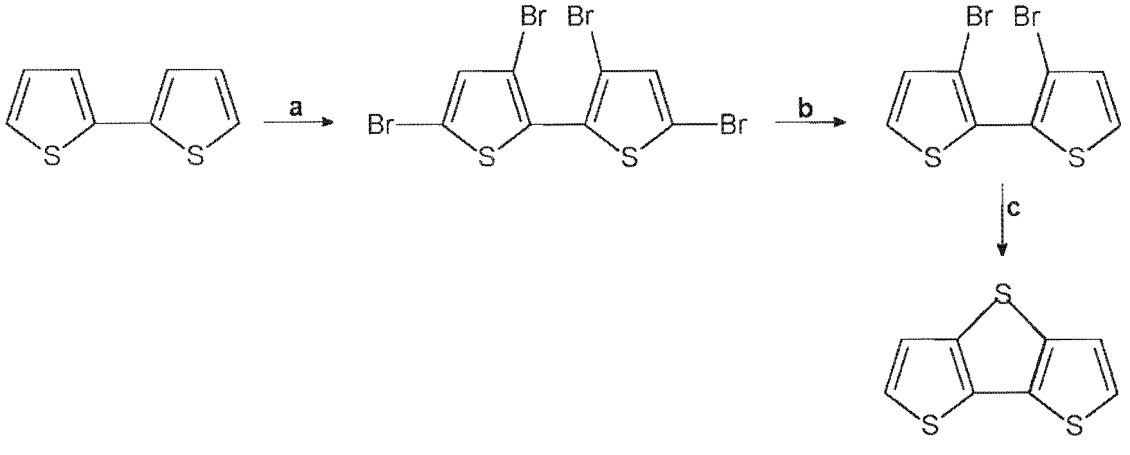

Figure 4.4 Reagents: **(a)** Br_2 (excess), reflux 24h; **(b)** Zn, reflux; **(c)** 2 eq. n-BuLi, SCl_2, THF, 0°C

2,2'-Bithiophene was treated with excess bromine to afford 3,3',5,5'-tetrabromo-2,2'-

[13] J.Ohshita, M. Nodono, T. Watanabe, Y. Ueno, A. Kunai, Y. Harima, K. Yamashita, M. Ishikawa, *J. Organomet. Chem.*, 553, **1998**, 487.

bithiophene[14]. Reaction of this tetrabromo product with zinc dust at elevated temperatures resulted in selective α-debromination to yield 3,3'-dibromo-2,2'-bithiophene. Lithiation of 3,3'-dibromo-2,2'-bithiophene with n-butyllithium, followed by the reaction with sulfur dichloride[15], afforded the target product, but unfortunately the desired compound was dissolved in a viscous oil which formed as byproduct. All attempts to separate the two products failed and this method was also found to be unsatisfactory.

In an final attempt to synthesize dithieno[3,2-*b*:2',3'-*d*]thiophene a combination of the methods described by De Jong *et al*[4] and Brandsma *et al*[15] was employed. 3-Bromothiophene was lithiated and the 3-lithiothiophene species was reacted with sulfur dichloride to yield di(3-thienyl)sulphide. Ring closure of this compound, using n-butyllithium followed by $CuCl_2$, gave dithieno[3,2-*b*:2',3'-*d*]thiophene (**I**) in low yields.

Seeing that the ring closure reaction was the most problematic step in the synthesis of the ligand, it was inferred that the lithiation of di(3-thienyl)sulphide was incomplete and that this was the reason for the failure in obtaining the target product. To establish whether this speculation had any credibility, a test reaction was conducted. After the dimetallation of di(3-thienyl)sulphide, one equivalent of tungsten hexacarbonyl was added, followed by the alkylation of the resulting dilithium salt with Et_3OBF_4. A green biscarbene complex **21** (figure 4.5) was yielded, refuting the assumption. The system for numbering of the atoms for characterization purposes is shown. Interestingly, no coordination of the linking sulfur atom was observed whereby two five-membered rings would result in a tricarbonyl complex. The infrared data supported a tetracarbonyl complex and a molecular ion peak at m/z = 660 confirmed a mononuclear complex.

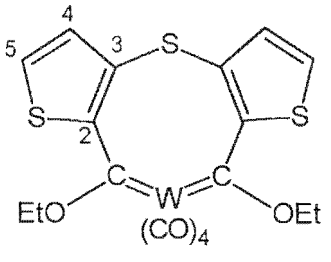

Figure 4.5 Structure of complex **21**

[14] S.C. Ng, H.S.O. Chan, H.H. Huang, R.S.H. Seow, *J. Chem. Res. (M)*, **1996**, 1285.

[15] L. Brandsma, H. Verkruijsse, *Preparative Polar Organometallic Chemistry I*, Springer-Verlag, Berlin Heidelberg, **1987**, p.162.

3. Synthesis of carbene complexes of Dithieno[3,2-*b*:2',3'-*d*]thiophene

On comparing the σ^+-values of the different positions of dithieno[3,2-*b*:2',3'-*d*]thiophene (figure 4.6), it is evident that the 2- and 9-positions are the most reactive. This was confirmed by electrophilic substitution studies done on the different dithienothiophene isomers by Archer and Taylor[8]

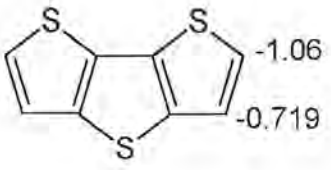

Figure 4.6 σ^+-values

Dimetallation of dithieno[3,2-*b*:2',3'-*d*]thiophene was effected according to the method employed by Brandsma *et al* for the dimetallation of thiophene[16]. This metallation involved the use of n-butyllithium and TMEDA in hexane at elevated temperatures. Deprotonation of dithieno[3,2-*b*:2',3'-*d*]thiophene, by using two equivalents of n-butyllithium to one equivalent of substrate, occurred at positions 2 and 9.

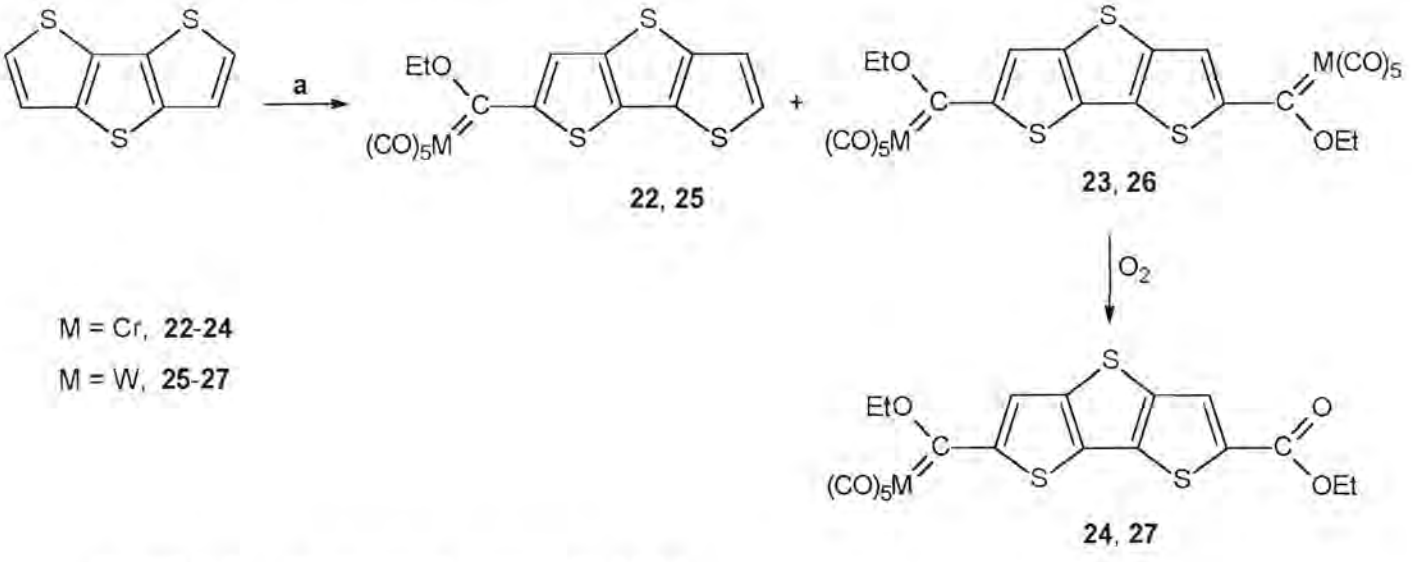

Figure 4.7 Synthesis of complexes **22-27**

Reagents: **a**(i) 2 eq. n-BuLi (ii) $ML_3(CO)_3$ (iii) $Et_3O\,BF_4$

[16] L. Brandsma, H. Verkruijsse, *Preparative Polar Organometallic Chemistry I*, Springer-Verlag, Berlin Heidelberg, **1987**, p.164.

Carbene complexes of chromium, tungsten and molybdenum were afforded employing the general Fischer method described in Chapter **2**. Upon reaction of $Cr(CO)_6$ with the dimetallated species and subsequent quenching with the alkylating agent, three products were afforded *i.e.* the orange monocarbene complex **22**, the purple biscarbene complex **23** as well as the pink-orange decomposition product, complex **24**. Three analogous compounds were yielded upon reaction with tungsten hexacarbonyl. Complexes **25**, **26** and **27** were isolated with column chromatography. The general synthetic procedure for the formation of these complexes is given in figure 4.7. The reaction between molybdenum hexacarbonyl and the dimetallated species afforded, after alkylation, three products. The first was the orange-red monocarbene complex, **28**, while the biscarbene complex **29** had a purple colour. The third purple-pink product that was isolated, complex **30**, was not the expected decomposition product, but was instead characterized as a biscarbene product formed by a carbene-carbene coupling reaction (figure 4.8).

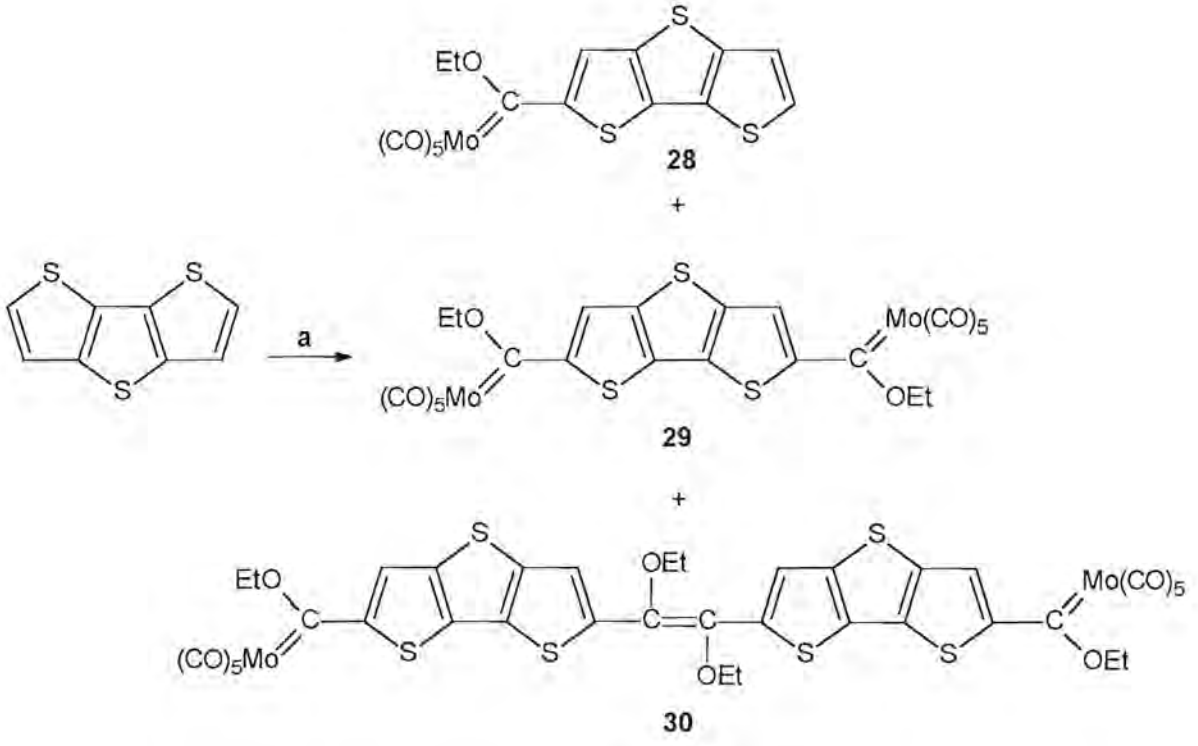

Figure 4.8 Synthesis of complexes **28-30**
Reagents: **a**(i) 2 eq. n-BuLi (ii) $M(CO)_6$ (iii) $Et_3O{\cdot}BF_4$

This biscarbene complex contained an extended conjugated bridging ligand. The difference between the formation of this product and the normal decomposition product is illustrated in figure 4.9. The formation of complex **28** constitutes the reaction between two biscarbene complexes, resulting in C-C bond formation and the elimination of a molybdenum species, yielding a growing biscarbene complex. This product has the possibility of, on repeating this process, forming a growing conducting polymer.

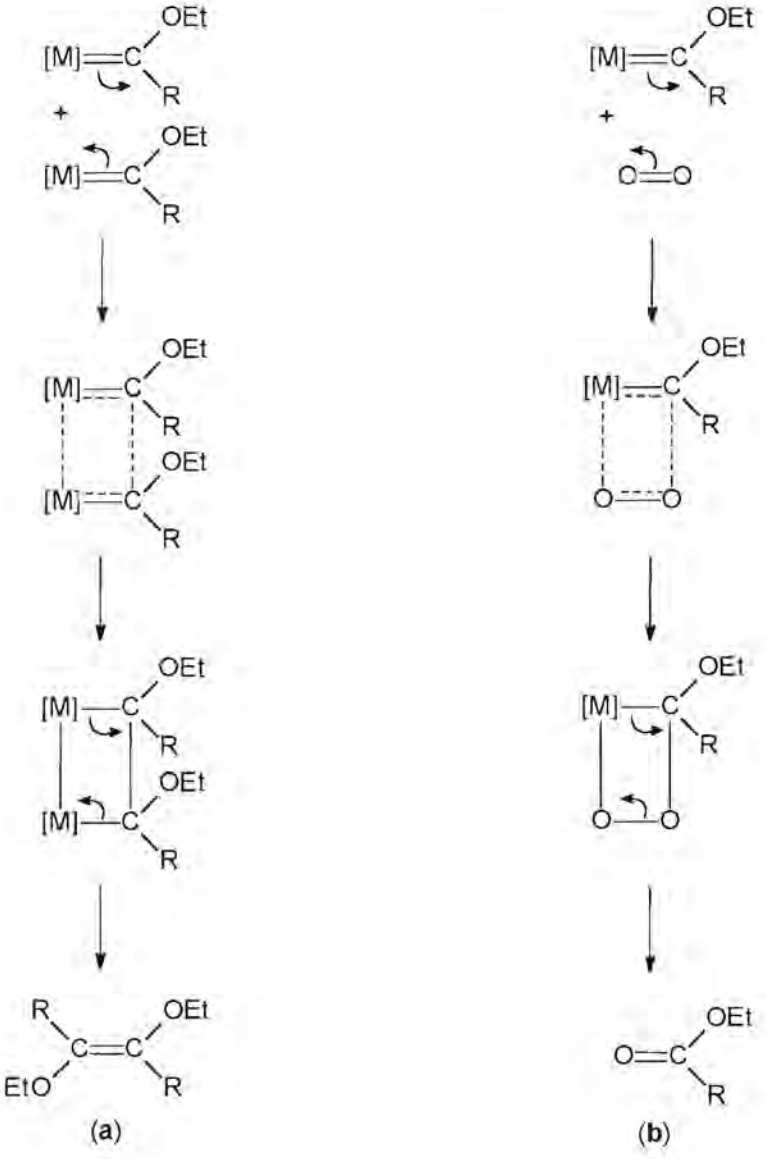

R = dithieno[3,2-*b*;2',3'-*d*]thiophene

Figure 4.9 Formation of (**a**) complex **30** and (**b**) decomposition products **24** and **27**

3.1 Spectroscopic characterization of novel carbene complexes

The carbene complexes were characterized using NMR and infrared spectroscopy and mass spectrometry. Confirmation of the molecular structures of compounds **22**, **23** and **27** were obtained from single crystal X-ray diffraction studies.

3.1.1 ^{1}H NMR spectroscopy

All NMR spectra were recorded in deuterated chloroform as solvent unless otherwise specified. The ^{1}H NMR data for complexes **22-30** are summarized in tables 4.1, 4.2 and 4.3.

Table 4.1 ^{1}H NMR data of complexes 22-24

Proton	Chemical shifts (δ, ppm) and Coupling constants (J, Hz)					
	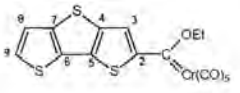 **22**		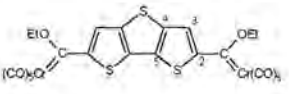 **23**		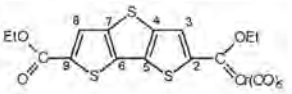 **24**	
	δ	J	δ	J	δ	J
H3	8.42 (s)	-	8.38 (s)	-	8.41 (s)	-
H8	7.32 (d)	5.2	-	-	8.00 (s)	-
H9	7.57 (d)	5.2	-	-	-	-
O**CH$_2$**CH$_3$-M	5.17 (q)	7.0	5.20 (q)	7.0	5.19 (q)	7.0
O**CH$_2$**CH$_3$-O	-	-	-	-	4.40 (q)	7.0
OCH$_2$**CH$_3$**-M	1.68 (t)	7.0	1.69 (t)	7.0	1.69 (t)	7.0
OCH$_2$**CH$_3$**-O	-	-	-	-	1.40 (t)	7.0

In the ^{1}H NMR spectrum of complex **21** two broad singlet peaks are observed for protons H4 and H5 at δ 7.30 and 7.58 ppm respectively. The O**CH$_2$**CH$_3$ protons are observed at 4.51 ppm as a quartet but again the resolution was not satisfactory. This value is lower than the normal biscarbene values observed in similar complexes, indicating that the protons are more shielded in this case. It is thus suggested that the carbene moieties are less electrophilic due to the influence of both moieties on one metal fragment instead of being bonded to two separate metal fragments. A $J^3_{H\text{-}H}$ coupling constant of 7.5 Hz was calculated for coupling to the methyl protons. Two triplet signals were observed at 1.72 and 1.60 ppm for the two OCH$_2$**CH$_3$** groups

since this is a fluxional molecule and the two ethoxy groups are free to rotate. Therefore they are in different chemical environments and two independent peaks are observed.

The chemical shift values, recorded in deuterated chloroform, for uncoordinated dithieno[3,2-*b*:2',3'-*d*]thiophene are 7.34 (H2, H9) and 7.27 (H3, H8). It is evident from the data in tables 4.1-4.3 that the coordination of metal moieties to the ligand has a significant influence on the electronic distribution of the complex. The substantial chemical shift differences for protons H3 and H8 on the spectra of the biscarbene complexes and the decomposition complexes compared to that of DTT indicate that the electrophilic carbene-metal moiety withdraws electron density from the ring, deshielding the protons on the ring and causing a downfield shift. On the spectra of the monocarbene complexes a similar trait is noticed and it is interesting to note that the protons furthest away from the metal fragment, H9 and, to a lesser extent, H8, are likewise affected due to conjugation in the ring system.

Table 4.2 **^{1}H NMR data of complexes 25-27**

Proton	Chemical shifts (δ, ppm) and Coupling constants (J, Hz)					
	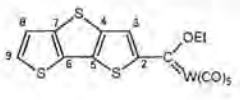 **25**		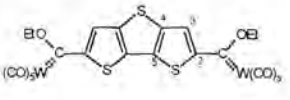 **26**		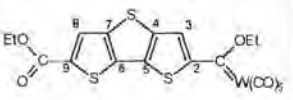 **27**	
	δ	J	δ	J	δ	J
H3	8.35 (s)	-	8.29 (s)	-	8.32 (s)	-
H8	7.31 (d)	5.2	8.29 (s)	-	8.00 (s)	-
H9	7.59 (d)	5.2	-	-	-	-
O**CH$_2$**CH$_3$-M	4.99 (q)	7.0	5.00 (q)	7.2	5.00 (q)	7.0
O**CH$_2$**CH$_3$-O	-	-	-	-	4.40 (q)	7.2
OCH$_2$**CH$_3$**-M	1.66 (t)	7.0	1.68 (t)	7.0	1.67 (t)	7.0
OCH$_2$**CH$_3$**-O	-	-	-	-	1.40 (t)	7.0

On comparing the chemical shift values of the methylene protons of the ethoxy groups of the carbenes for different metal complexes, it seems to make little difference whether the ligand is coordinated to one or two carbene-metal moieties. It appears however that the chemical shift values are affected by the nature of the metal fragment. Characteristic values are observed for chromium, while the values for molybdenum are slightly lower and the chemical shifts for

the tungsten complexes are observed upfield compared to the other metal complexes. The chemical shift values obtained for the novel carbene metal complexes correspond well with values obtained in literature. Values for the ethoxy protons of the chromium and tungsten monocarbene carbene complexes with thiophene as bridging unit were reported as 5.16, 1.65 ppm and 4.99, 1.64 ppm respectively[17]. The spectra of the biscarbene analogues of these complexes[18] displayed values of 5.21, 1.69 ppm (Cr) and 4.98, 1.68 ppm (W). The proton spectrum of complex **27** is depicted in figure 4.10. The analogous molybdenum decomposition product of complexes **24** (Cr) and **27** (W) was only observed in a very low yield on TLC. This product could not be isolated.

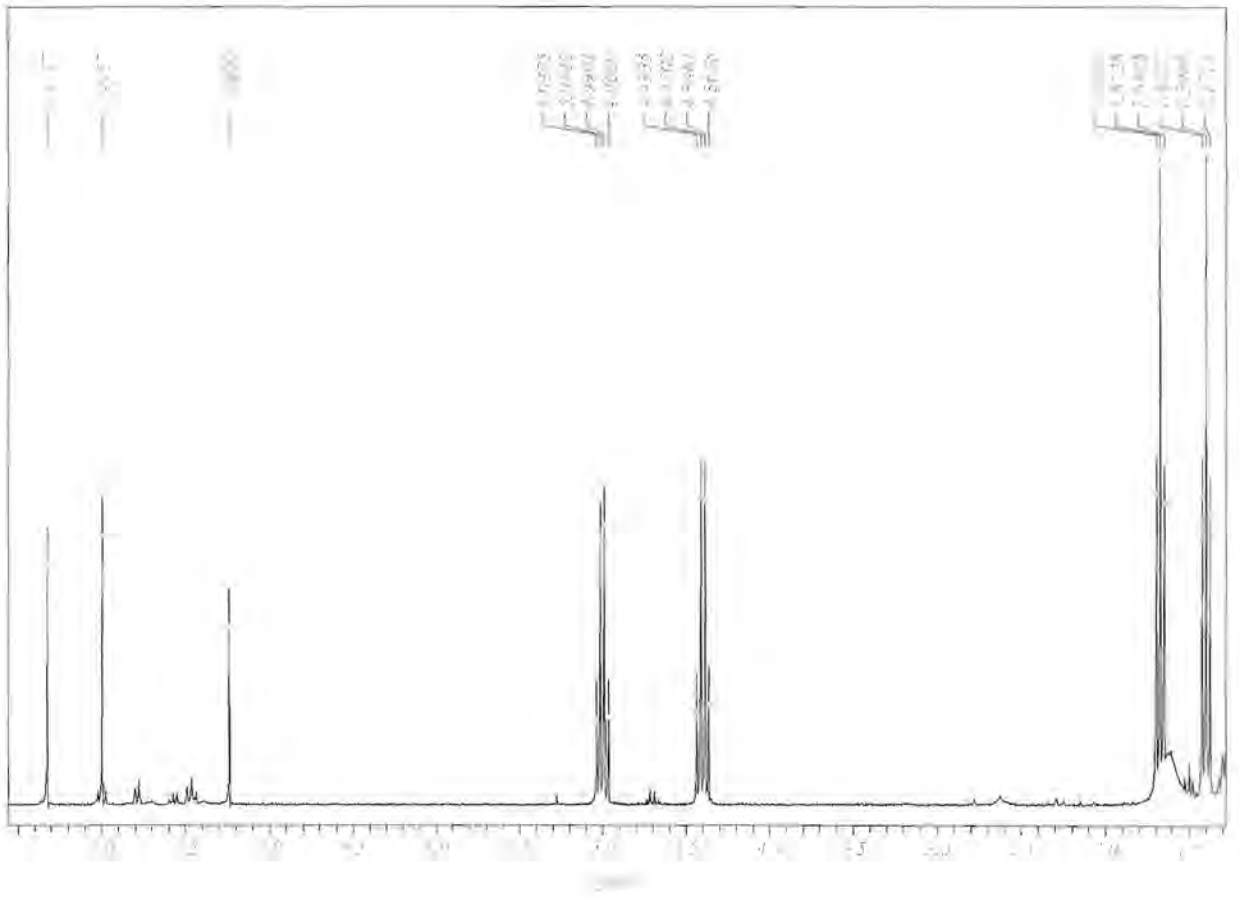

Figure 4.10 Proton spectrum of the tungsten decomposition product, complex **27**

[17] M.Y. Darensbourg, D.J. Darensbourg, *Inorg. Chem.*, 9, **1970**, 32.

[18] Y.M. Terblans, H.M. Roos, S. Lotz, *J. Organomet. Chem.*, 566, **1998**, 133.

Indication of the existence of this decomposition product can be found on the spectrum of complex **30**, where the small quartet at 4.35 ppm is associated with the methylene protons of the ester functionality of this product. The main pattern of decomposition, instead, leads to a carbene-carbene coupling reaction of the biscarbene complex **29** to yield an extended spacer. Characteristic for **30** is the intensity ratio of the methylene resonances and the chemical shift at 4.00 ppm. This again highlights differences in the chemistry of biscarbene complexes of molybdenum compared to chromium and tungsten.

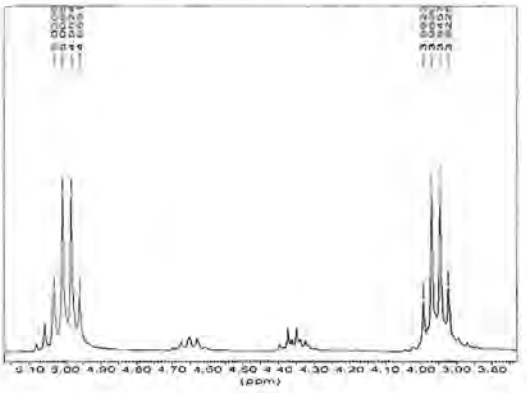

Figure 4.11 Methylene region on the ^{1}H NMR spectrum of complex **30**

Table 4.3 **^{1}H NMR data of complexes 28-30**

Proton	Chemical shifts (δ, ppm) and Coupling constants (J, Hz)					
	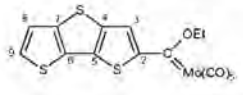 **28**		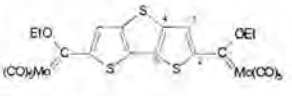 **29**		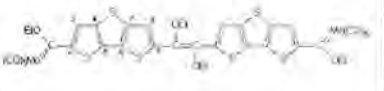 **30**	
	δ	J	δ	J	δ	J
H3	8.38 (s)	-	8.33 (s)	-	8.34 (s)	-
H8	7.33 (d)	5.2	-	-	7.28 (s)	-
H9	7.59 (d)	5.4	-	-	-	-
O**CH$_2$**CH$_3$-M	5.07 (q)	7.1	5.09 (q)	7.0	5.04 (q)	7.4
O**CH$_2$**CH$_3$-O	-	-	-	-	4.00 (q)	7.0
OCH$_2$**CH$_3$**-M	1.66 (t)	7.0	1.68 (t)	7.1	1.63 (t)	7.0
OCH$_2$**CH$_3$**-O	-	-	-	-	1.40 (t)	7.0

3.1.2 ^{13}C NMR spectroscopy

The ^{13}C NMR data of complexes **22-30** are given in table 4.4.

Table 4.4 ^{13}C NMR data of complexes 22, 23, 24, 25, 27, 28, 29 and 30

Carbon	Chemical shifts (δ, ppm)							
	22	**23**	**24**	**25**	**27**	**28**	**29**	**30**
	δ	δ	δ	δ	δ	δ	δ	δ
Carbene	312.0	314.8	314.4	286.7	288.6	302.6	n.o.	302.3
C2	154.4	157.5	161.9	158.0	161.9	n.o.	156.1	155.7
C3	135.0	133.4	134.1	135.6	134.7	135.6	133.7	135.3
C4, C5, C6, C7	142.8 146.8	137.0 146.1	137.7 140.9 144.6 145.1	142.6 146.0	132.4 137.8 138.3 145.3	142.6 147.0	136.2 146.8	138.5 139.2 142.7 142.8
C8	121.1	-	126.6	121.2	126.7	121.1	-	122.1
C9	130.7	-	156.2	130.9	159.6	130.9	-	146.6
O**CH**$_2$CH$_3$ -M	75.8	76.2	76.1	78.2	78.5	77.2	77.9	77.4
O**CH**$_2$CH$_3$ -O	-	-	61.8	-	61.9	-	-	67.5
OCH$_2$**CH**$_3$ -M	15.2	15.1	15.2	15.0	14.9	15.1	15.0	15.1
OCH$_2$**CH**$_3$ -O	-	-	14.3	-	14.3	-	-	15.6
M(CO)$_5$	217.1 (*cis*) 223.2 (*trans*)	216.8 (*cis*) 223.2 (*trans*)	216.9 (*cis*) 223.2 (*trans*)	197.6 (*cis*) 202.3 (*trans*)	197.4 (*cis*) 202.3 (*trans*)	206.1 (*cis*) 212.7 (*trans*)	205.9 (*cis*) 212.1 (*trans*)	206.1 (*cis*) 212.7 (*trans*)
C=O	-	-	n.o.	-	198.2	-	-	-
C-OEt	-	-	-	-	-	-	-	108.1

On the ^{13}C NMR spectrum of complex **21** the carbene peak was observed at δ 290.8 ppm. This value correlates well with values determined for the novel tungsten monocarbene complexes

as well as literature values[19]. This value supports the deduction made from the ^{1}H NMR data that the carbene carbon is less electrophilic in this complex and the carbene carbon therefore more shielded. Two signals were obtained for the tetracarbonyl-metal moiety at 212.4 ppm and 204.5 ppm, corresponding to the CO_{trans} and CO_{cis} carbonyl ligands respectively. The quaternary carbon signal at 158.0 ppm was assigned to C2 while the peak for C3 was observed at 139.1 ppm. Signals for C4 and C5 were found at 129.8 and 121.3 ppm, the higher value being assigned to C5 due to its position next to the heteroatom. On the spectrum two different signals are observed for the carbons of the two ethoxy groups. Again, confirming the ^{1}H NMR data, it is concluded that the two ethoxy groups are in different chemical environments. The chemical shift values for the two -O**C**$H_2$$CH_3$ are 79.7 and 79.4 ppm and for the methyl groups are 14.8 and 14.1 ppm. From these values as well as the other proton NMR data it is clear that the methyl groups are for some unknown reason more affected than the -O**C**$H_2$$CH_3$ groups, since the chemical shift difference is more prominent. A crystal structure could throw light on this observation, but all attempts to isolate crystals suitable for X-ray structural studies, unfortunately, failed.

The ^{13}C NMR spectrum of complex **26** was of an unsatisfactory quality since the poor solubility of the product in $CDCl_3$ prevented the acquisition of a decent data set. The following peaks (ppm) were observed on the spectrum and assigned to the different carbon atoms: 202.3 ($M(CO)_5$ *trans*); 197.6 ($M(CO)_5$ *cis*); 133.8 (C3); 78.6 (O**C**$H_2$$CH_3$-M); 14.9 ($OCH_2$**C**$H_3$-M). On many of the spectra a resonance peak at 182.2 ppm was observed. This peak was assigned to free CO which was released during the recording of the spectra and was dissolved by the solvent. The position of the methylene resonances as well as the methyl resonances of the ethoxy group were found to have characteristic values, depending on the functionality of adjacent groups. These values were consistent for all complexes irrespective of the number of conjugated thiophene moieties and, to a large extent, independent of the metal fragment (figure 4.12).

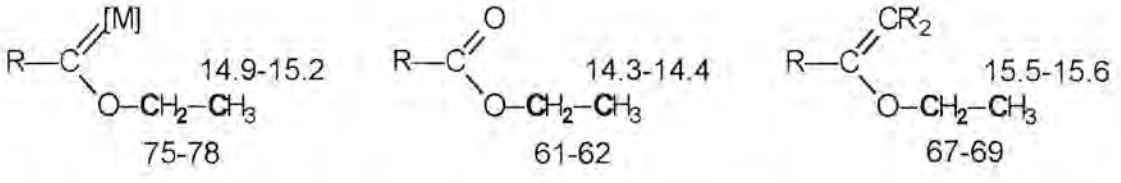

Figure 4.12 Characteristic positions of the ethoxy carbons on ^{13}C NMR spectra (ppm)

[19] E.O. Fischer, T. Selmayr, F.R. Kreissl, U. Schubert, *Chem. Ber.*, 110, **1977**, 2547.

Although the resonances of the methylene carbons are largely independent, a small difference is still noted for the different metal complexes. The methylene carbon peaks of the carbene ethoxy group on the spectra of the chromium complexes are all observed at 75.5-76.2 ppm, while the corresponding peaks were found at 78.2-78.9 ppm for the tungsten complexes and at 77.2-77.9 ppm for the molybdenum complexes. The trend is thus W > Mo > Cr, corresponding to the size of the metal atom and the relative positions of the metals on the periodic table. This same sequence is observed for the corresponding methyl carbons of the different metal complexes but in the opposite order.

3.1.3 Infrared Spectroscopy

The infrared data of complexes **22-30** are outlined in table 4.5.

Table 4.5 Infrared data[a] of complexes 22-30 in the carbonyl region

Band	Stretching vibrational frequency (ν_{CO}, cm^{-1})								
	22	**23**	**24**	**25**	**26**	**27**	**28**	**29**	**30**
$A_1^{(1)}$	2056	2054	2056	2064	2064	2066	2066 2066	2064 2066	2066 2066
B	1982	1979	1978	1976	1979	1979	1981 1989	1981 1989	1983 1989
$A_1^{(2)}$	1941	1944	1942	1937	1937	1939	1944 1950	1946 1954	1944 1952
E	1941	1944	1942	1937	1937	1939	1944 1950	1946 1954	1944 1952

[a] First set of values recorded in dichloromethane, second set in hexane

The IR spectrum of complex **21** was recorded in hexane and in dichloromethane. Since this is a tetracarbonyl-metal complex, four infrared active bands were observed in the carbonyl stretching frequency region. On the hexane spectrum four distinct bands can be distinguished, while degeneracy of the $A_1^{(2)}$ and B_1 bands occurs in dichloromethane and only three peaks are observed. On the spectrum recorded in hexane peaks were observed at the following wavenumbers: 2025 cm^{-1} ($A_1^{(1)}$), 1955 cm^{-1} ($A_1^{(2)}$), 1942 cm^{-1} (B_1) and 1889 cm^{-1} (B_2). The three bands on the spectrum recorded in dichloromethane were observed at 2022 cm^{-1} ($A_1^{(1)}$), 1944 cm^{-1} ($A_1^{(2)}$ and B_1) and 1869 cm^{-1} (B_2). These values correspond well with values obtained for

a similar tungsten biscarbene complex prepared by Fischer *et al*[20]. Values for the 1,4-chelated *o*-phenylene tetracarbonyl tungsten ethoxy biscarbene complex are only marginally higher than for complex **21** and are: 2032 cm^{-1} ($A_1^{(1)}$), 1957 cm^{-1} ($A_1^{(2)}$), 1947 cm^{-1} (B_1) and 1896 cm^{-1} (B_2).

The carbonyl vibration frequencies of the ester groups of complexes **24** and **27** were observed as lower intensity bands at 1650 cm^{-1} and 1652 cm^{-1}, respectively. This band was noticeably absent on the spectrum of complex **30**.

3.1.4 Mass spectrometry

The data for the fragmentation of complexes **21**-**28** are presented in table 4.6.

From the data in table 4.6 it is evident that the monocarbene complexes, biscarbene complexes and decomposition complexes have different fragmentation patterns respectively. The monocarbene complexes show initial fragmentation of five carbonyl groups followed by the loss of the ethyl group and eventually the elimination of the carbene carbonyl group. On the spectra of the biscarbene complexes the M^+ peaks were not observed. Instead, on all three spectra the M^+ - 4CO fragmentation peak was the peak observed at highest m/z-value. A definite fragmentation pattern for the biscarbene complexes could not be distinguished. However, certain discernable fragments could be identified which were present on all three spectra. The first meaningful peak was identified as the M^+ ion of the decomposition product i.e. one metal carbonyl fragment was replaced by an ester group. After this the consecutive loss of five carbonyl groups is observed and the peaks associated with these fragments could be assigned. Interestingly, the principal ion on all three spectra is found at a m/z value of 340, which corresponds to a fragment ion where both carbene fragments are replaced by ester groups. The fragmentation patterns of the decomposition products are very similar to that of the monocarbene complexes. The molecular ion peak was observed in all three cases and the fragmentation started with the stepwise loss of three carbonyl groups. In the spectrum of **24** the consequent loss of carbonyl groups ensued, while the elimination of the ethyl group preceded the further loss of the carbonyl groups in the spectrum of **27**.

[20] E.O. Fischer, W. Röll, N. Hoa Tran Huy, K. Ackermann, *Chem. Ber.*, 115, **1982**, 2951.

Table 4.6 Fragmentation patterns of complexes 21-28

Complex	Fragment ions (I, %)
21	606.2 (2) M^+; 578.1 (4) M^+ - CO; 550.1 (1) M^+ - 2CO; 522.2 (1) M^+ - 3CO; 494.2 (6) M^+ - 4CO; 465.1 (3) M^+ - 4CO - Et; 436.0 (12) M^+ - 4CO - 2Et; 408.9 (5) M^+ - 5CO - 2Et; 380.0 (6) M^+ - 6CO - 2Et
22	444.1 (8) M^+; 416.2 (19) M^+ - CO; 388.1 (15) M^+ - 2CO; 360.1 (11) M^+ - 3CO; 332.2 (43) M^+- 4CO; 304.1 (96) M^+- 5CO; 275.0 (72) M^+- 5CO - Et; 247.0 (81) M^+- 6CO - Et
23	580.1 (12) M^+ - 4CO; 516.2 (44) **24**$^+$; 488.3 (29), **24**$^+$ - CO; 460.2 (16) **24**$^+$ - 2CO; 432.2 (32) **24**$^+$ - 3CO; 404.2 (76) **24**$^+$ - 4CO; 376.2 (14) **24**$^+$ - 5CO
24	516.2 (1) M^+; 488.2 (2) M^+ - CO; 460.1 (2) M^+ - 2CO; 432.2 (1) M^+ - 3CO; 404.2 (8) M^+ - 4CO; 376.1 (36) M^+ - 5CO; 347.2 (17) M^+ - 5CO - Et; 319.1 (11) M^+ - 6CO - Et
25	576.2 (49) M^+; 548.2 (23) M^+- CO; 520.0 (27) M^+- 2CO; 491.2 (9) M^+- 3CO; 463.1 (71) M^+- 4CO; 435.1 (100) M^+- 5CO; 407.1 (51) M^+- 5CO -Et; 379.1 (87) M^+- 6CO -Et
26	844.2 (6) M^+ - 4CO; 648.1 (17) **27**$^+$; 620.2 (12) **27**$^+$ - CO; 592.0 (13) **27**$^+$ - 2CO; 564.0 (30) **27**$^+$ - 3CO; 536.1 (41) **27**$^+$ - 4CO; 508.2 (73) **27**$^+$ - 5CO
27	648.5 (32) M^+; 620.4 (16) M^+ - CO; 592.4 (24) M^+ - 2CO; 563.4 (8) M^+ - 2CO - Et; 535.4 (57) M^+ - 3CO - Et; 507.4 (83) M^+ - 4CO - Et; 479.4 (36) M^+ - 5CO - Et; 451.3 (67) M^+ - 6CO - Et
28	488.7 (5) M^+; 461.0 (13) M^+ - CO; 432.5 (2) M^+ - 2CO; 404.5 (7) M^+ - 3CO; 376.5 (8) M^+ - 4CO; 348.4 (32) M^+ - 5CO; 319.3 (6) M^+ - 5CO - Et; 291.3 (20) M^+ - 6CO - Et

3.1.5 X-ray Crystallography

Single crystal X-ray structure determinations confirmed the structures of complexes **22**, **23** and **27**. The crystals were afforded from dichloromethane:hexane (1:1) solutions for complexes **22** and **23** and from chloroform:hexane (1:1) solutions for complex **27**. Complex **22** crystallized as orange-red needles, while complex **23** afforded small, dark purple needle-like crystals. The crystals of complex **27** were orange needles. Figures 4.14, 4.15 and 4.17 represent ball-and-stick plots of the respective structures. Selected bond lengths and angles are given in tables 4.7, 4.8 and 4.10. The crystal structure of uncoordinated dithieno[3,2-*b*:2',3'-*d*]thiophene was determined by Bertinelli *et al*[21]. In figure 4.13 the determined bond lengths and angles are indicated for this compound.

[21] F. Bertinelli, P. Palmieri, C. Stremmenos, G. Pelizzi, C. Taliani, *J. Phys. Chem.*, 87, **1983**, 2317.

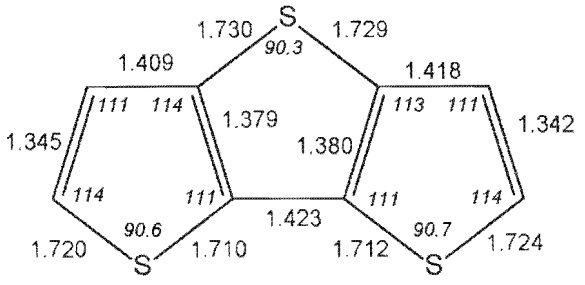

Figure 4.13 Bond lengths (Å) and bond angles (°) of dithieno[3,2-*b*:2',3'-*d*]thiophene

3.1.5.1 Crystal structure of complex 22

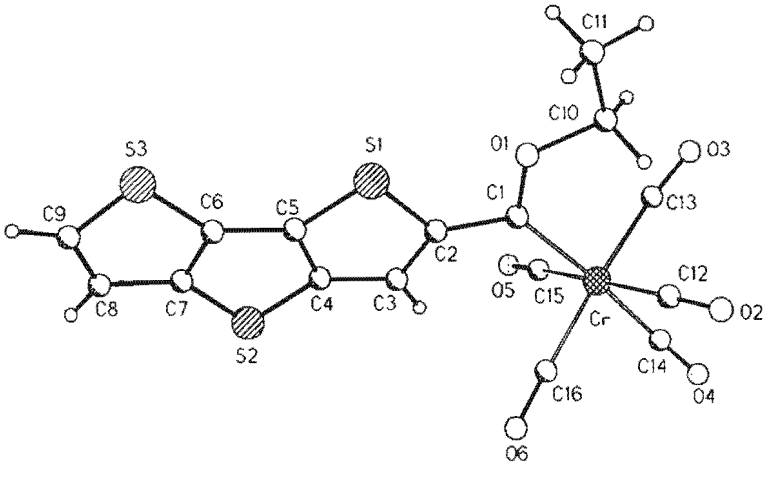

Figure 4.14 Ball-and-stick plot of complex **22**

The Cr metal is in the centre of an octahedral ligand environment in complex **22**. The heteroaromatic ring system in the structure is planar and in the same plane as the carbene carbon and the metal atom. The metal moiety is orientated away from the sulfur atom on the opposite side of the ring, similar to the structures obtained for complexes **1**, **19** and structures of similar thiophene complexes reported in literature[18]. The bond lengths of the ring system in complex **22** are all longer or similar to the bond lengths determined for the same bonds in the structure of the dithienothiophene[21]. It is therefore assumed that the effect of delocalization is present in this structure as was indicated for the structures of the complexes discussed in Chapter **3**. Bond angles of the dithienothiophene ring in the complex differ slightly from the literature values for DTT, indicating distortion of the rings on coordination to the carbene moiety.

Table 4.7 Selected bond lengths and angles of complex 22

22	Bond lengths (Å)	22	Bond angles (°)
Cr-C(1)	2.091(7)	C(5)-S(1)-C(2)	91.2(3)
S(1)-C(5)	1.722(7)	C(7)-S(2)-C(4)	89.4(3)
S(1)-C(2)	1.765(7)	C(9)-S(3)-C(6)	90.1(4)
S(2)-C(4)	1.765(7)	C(1)-O(1)-C(10)	123.3(5)
S(2)-C(7)	1.742(8)	O(1)-C(1)-C(2)	105.2(6)
S(3)-C(9)	1.727(8)	O(1)-C(1)-Cr	129.3(5)
S(3)-C(6)	1.729(7)	C(2)-C(1)-Cr	125.5(5)
O(1)-C(1)	1.332(8)	C(3)-C(2)-S(1)	111.3(5)
O(1)-C(10)	1.457(8)	C(2)-C(3)-C(4)	111.1(6)
C(1)-C(2)	1.448(9)	C(5)-C(4)-C(3)	114.9(6)
C(2)-C(3)	1.401(9)	C(5)-C(4)-S(2)	112.7(5)
C(3)-C(4)	1.403(10)	C(4)-C(5)-C(6)	112.3(6)
C(4)-C(5)	1.380(10)	C(4)-C(5)-S(1)	111.5(5)
C(5)-C(6)	1.427(10)	C(7)-C(6)-C(5)	112.0(7)
C(6)-C(7)	1.383(10)	C(7)-C(6)-S(3)	111.2(5)
C(7)-C(8)	1.444(10)	C(6)-C(7)-C(8)	114.2(7)
C(8)-C(9)	1.353(12)	C(6)-C(7)-S(2)	113.5(5)
		C(9)-C(8)-C(7)	108.7(7)
		C(8)-C(9)-S(3)	115.8(6)

3.1.5.2 Crystal structure of complex 23

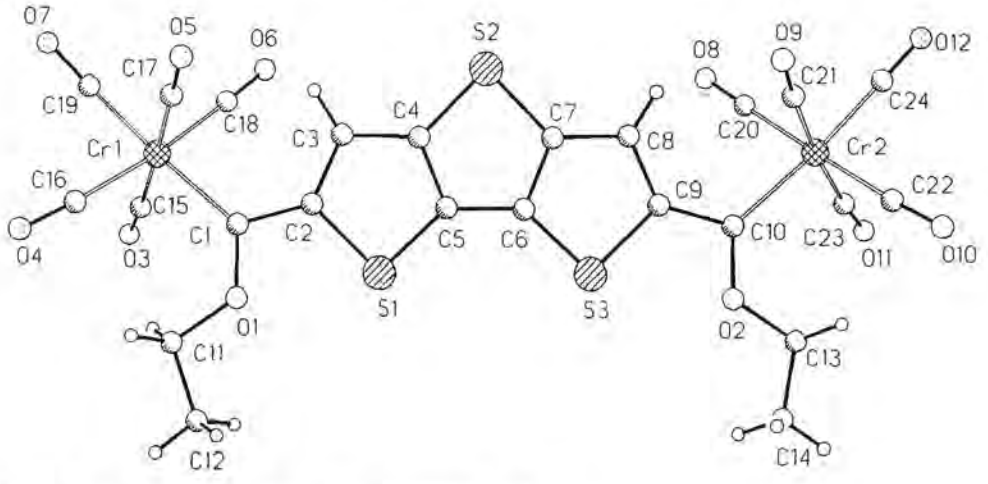

Figure 4.15 Ball-and-stick plot of complex **23**

A plane of symmetry is found in complex **23** which is perpendicular to the bridging ligand, intersecting S(2) and bisecting the C(5)-C(6) bond of the ring. The additional ring places the metal fragments on the same side of the line connecting the two carbene carbons.

Table 4.8 Selected bond lengths and angles of complex 23

23	Bond lengths (Å)	23	Bond angles (°)
Cr(1)-C(1)	2.051(9)	C(5)-S(1)-C(2)	91.2(4)
Cr(2)-C(10)	2.077(9)	C(7)-S(2)-C(4)	89.3(4)
S(1)-C(5)	1.727(8)	C(9)-S(3)-C(6)	91.5(4)
S(1)-C(2)	1.760(8)	C(1)-O(1)-C(11)	123.5(7)
S(2)-C(7)	1.740(8)	C(10)-O(2)-C(13)	123.8(7)
S(2)-C(4)	1.744(8)	O(1)-C(1)-C(2)	104.2(7)
S(3)-C(6)	1.713(9)	O(1)-C(1)-Cr(1)	130.1(6)
S(3)-C(9)	1.776(8)	C(2)-C(1)-Cr(1)	125.7(6)
O(1)-C(1)	1.333(10)	O(2)-C(10)-C(9)	105.9(7)
O(2)-C(10)	1.327(10)	O(2)-C(10)-Cr(2)	130.1(6)
O(1)-C(11)	1.474(10)	C(9)-C(10)-Cr(2)	124.0(6)
O(2)-C(13)	1.457(11)	C(3)-C(2)-S(1)	111.1(6)
C(1)-C(2)	1.454(11)	C(2)-C(3)-C(4)	112.3(8)
C(9)-C(10)	1.460(12)	C(5)-C(4)-C(3)	113.2(7)
C(2)-C(3)	1.396(11)	C(5)-C(4)-S(2)	113.5(6)
C(3)-C(4)	1.415(11)	C(4)-C(5)-C(6)	112.7(7)
C(4)-C(5)	1.384(11)	C(4)-C(5)-S(1)	112.1(6)
C(5)-C(6)	1.426(12)	C(7)-C(6)-C(5)	110.4(8)
C(6)-C(7)	1.405(11)	C(7)-C(6)-S(3)	112.2(6)
C(7)-C(8)	1.407(12)	C(6)-C(7)-C(8)	112.7(8)
C(8)-C(9)	1.393(12)	C(6)-C(7)-S(2)	114.1(6)
		C(9)-C(8)-C(7)	113.3(8)
		C(8)-C(9)-S(3)	110.3(6)

In table 4.9 literature values are reported for bond lengths of similar chromium mono- and biscarbene complexes as well as selected bond lengths of complexes **8**, **9** and **19**.

Table 4.9 Literature values

Complex	Bond length (Å)				Reference
	$M\text{-}C_{carbene}$	$C_{carbene}\text{-}O$	O-R	$C_{carbene}\text{-}R'$	
$Cr(CO)_5C(OMe)Ph$	2.04(3)	1.33(2)	1.46	1.47(4)	[22]
$Cr(CO)_5C(OEt)Me$	2.05(1)	1.31(1)	-	1.51(1)	[23]
$Cr(CO)_5C(OH)Ph$	2.05(1)	1.32(1)	-	-	[24]
$Cr(CO)_5C[OSi(SiMe_3)_3]$1-furyl	2.03(1)	1.32(1)	-	1.45(1)	[25]
$[\{Cr(CO)_5C(OEt)\}_2T]$	2.04(1)	1.32(1)	1.45(1)	1.47(1)	[18]
$[\{Cr(CO)_5C(OEt\}_2$biphenylene]	2.05(1)	1.32(1)	-	1.49(1)	[26]
Complex **8**	2.08(1)	1.32(1)	1.46(1)	1.47(1)	-
Complex **9**	2.07(1)	1.33(1)	1.45(1)	1.47(1)	-
Complex **19**	2.06(1)	1.34(1)	1.47(1)	1.46(1)	-

The bond distances of the C(2)-S(1) and C(9)-S(3) bonds are markedly longer than the rest of the C-S bonds of the ring system. This implies that these two bonds are the most affected by the coordination of DTT to the metal-carbene moieties and that the delocalization of the electron density in the ring excludes the sulfur atoms of the ring (figure 4.16). This effect is supported by the longer metal-carbene carbon bonds (2.08(1) Å av) and shorter C(1)-C(2) bond (1.45(1) Å av), since a normal C-C (single bond) is 1.51(3) Å[27].

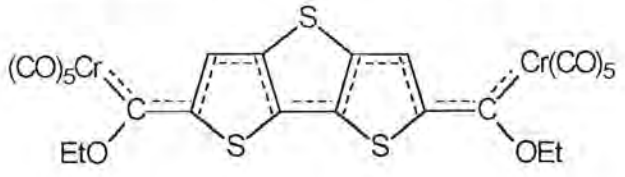

Figure 4.16 Delocalization of electron density in complex **23**

---

[22] U. Schubert, *Organometallics*, 1, **1982**, 1085.

[23] K.H. Dötz, H. Fischer, P.Hofmann, F.R. Kreissl, U. Schubert, K. Weiss, *Transition Metal Carbene Complexes*, VCH Verlag, Weinheim, **1983**, p.94.

[24] R.J. Klinger, J.C. Huffman, J.K. Kochi, *Inorg. Chem.*, 20, **1981**, 34.

[25] U. Schubert, M. Wiener, F.H. Köhler, *Chem. Ber.*, 112, **1979**, 708.

[26] N.H. Tran Huy, P. Lefloch, F. Robert, J. Jeannin, *J. Organomet. Chem.*, 327, **1987**, 211.

[27] F.A. Cotton, C.M. Lukehart, *Prog. Inorg. Chem.*, 16, **1972**, 487.

In literature[28], the value obtained for a C(sp^2)-C(aryl) bond for a conjugated arene was 1.470 Å and for an unconjugated arene 1.488 Å.

The angles O(1)-C(1)-C(2), O(1)-C(1)-Cr(1) and C(2)-C(1)-Cr(1) of 104.2(7)°, 130.1(6)° and 125.7(6)° respectively are typical for Fischer carbene complexes[29]. These values are similar to the values obtained for chromium complexes **8**, **9**, **19** and **22**.

3.1.5.3 Crystal structure of complex 27

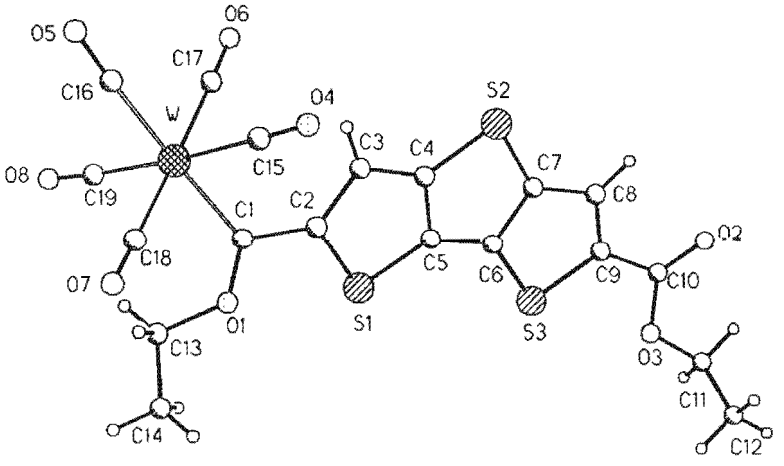

Figure 4.17 Ball-and-stick plot of complex **27**

The ethoxy group of the ester functionality in complex **27** is orientated towards the sulfur atom of the ligand, similar to the position inhabited by the ethoxy group on the carbene carbon. The bond angles surrounding C10, the carbon associated with the ester moiety, were determined as O(2)-C(10)-C(9) 123.5(8)°, O(3)-C(10)-C(9) 111.6(7)° and O(2)-C(10)-O(3) 124.9(8)° while the similar bond angles around the carbene carbon C(1) were found to be O(1)-C(1)-C(2) 105.2(7)°, O(1)-C(1)-W 130.2(5)° and C(2)-C(1)-W 124.6(6)°.

Delocalization of the electron density is evident in the lengthening of the C(2)-C(3) and C(4)-

---

[28] F.H. Allen, O. Kennard, D.G. Watson, L. Brammer, A.G. Orpen, R. Taylor, *J. Chem. Soc., Perkin 2*, **1987**, S1.

[29] U. Schubert, *Coord. Chem. Rev.*, 55, **1984**, 261.

C(5) bonds of 1.400(11) Å and 1.406(11) Å, the latter is now comparable with the bond length of 1.405(10) Å for C(3)-C(4). This delocalization diminishes on proceeding to the next ring fragment, moving further away from the metal-carbene moiety. This implies that the ester functionality does not contribute much to the delocalization of the ring.

Table 4.10 Selected bond lengths and angles of complex 27

27	Bond lengths (Å)	27	Bond angles (°)
W-C(1)	2.194(9)	C(5)-S(1)-C(2)	91.3(4)
S(1)-C(5)	1.729(7)	C(7)-S(2)-C(4)	89.5(4)
S(1)-C(2)	1.765(8)	C(9)-S(3)-C(6)	90.6(4)
S(2)-C(4)	1.739(7)	C(1)-O(1)-C(13)	121.3(6)
S(2)-C(7)	1.747(8)	O(1)-C(1)-C(2)	105.2(7)
S(3)-C(6)	1.718(8)	O(1)-C(1)-W	130.2(5)
S(3)-C(9)	1.746(8)	C(2)-C(1)-W	124.6(6)
O(1)-C(1)	1.332(10)	C(3)-C(2)-S(1)	111.1(6)
O(1)-C(13)	1.445(8)	C(2)-C(3)-C(4)	112.7(7)
O(2)-C(10)	1.206(9)	C(5)-C(4)-C(3)	113.3(7)
C(1)-C(2)	1.488(10)	C(5)-C(4)-S(2)	113.4(6)
C(9)-C(10)	1.477(11)	C(4)-C(5)-C(6)	111.9(7)
C(2)-C(3)	1.400(11)	C(4)-C(5)-S(1)	111.6(6)
C(3)-C(4)	1.405(10)	C(7)-C(6)-C(5)	111.5(7)
C(4)-C(5)	1.406(11)	C(7)-C(6)-S(3)	111.7(6)
C(5)-C(6)	1.416(10)	C(6)-C(7)-C(8)	112.5(8)
C(6)-C(7)	1.401(11)	C(6)-C(7)-S(2)	113.6(6)
C(7)-C(8)	1.426(11)	C(9)-C(8)-C(7)	111.8(7)
C(8)-C(9)	1.349(12)	C(8)-C(9)-S(3)	113.4(6)

5 Iron complexes of Thiophene derivatives

1. General

Organometallic complexes in which two metal-containing fragments are bridged by arene or heteroarene ligands can serve as models for repeating units in related organometallic polymers[1,2]. By increasing the number of fused aromatic rings in the bridging group of such material, the degree of intermetallic conjugation is expected to increase in complexes having two metal centres σ-bonded to the rings[3]. To determine the magnitude of this effect, Hunter *et al*[4] studied fused heteroarene ligands substituted by $FeCp(CO)_2$-moieties and derivatives thereof. Heteroarene ligands used in this study included quinoline, quinazoline and quinoxaline, all compounds containing a nitrogen atom in the aromatic system. The new complexes were prepared by reacting $Na[FeCp(CO)_2]$ with the heterocyclic compounds containing halide substituents at low temperatures. Nucleophilic displacement takes place as the more activated chlorine atoms bonded to the heteroarene ring is displaced by the strong $[FeCp(CO)_2]^-$ nucleophiles (figure 5.1).

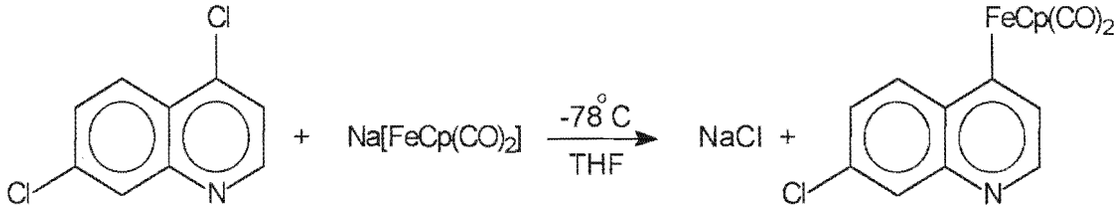

Figure 5.1 Synthesis of a monosubstituted quinoline complex

---

[1] R. McDonald, K.C. Sturge, A.D. Hunter, L. Shilliday, *Organometallics*, 11, **1992**, 893.

[2] X.A. Guo, K.C. Sturge, A.D. Hunter, M.C. Williams, *Macromolecules*, 27, **1994**, 7825.

[3] A.D. Hunter, D. Ristic-Petrovic, J.L. McLernon, *Organometallics*, 11, **1992**, 864.

[4] A.D. Hunter, R. Chukwu, B.D. Santarsiero, S.G. Bott, J.L. Atwood, *J. Organomet. Chem.*, 526, **1996**, 1.

Mono- and disubstituted products were prepared in this fashion.

The reaction of the iron complex $[FeCp(CO)_2(\eta^2\text{-propene})]Cl$ in a diethyl ether suspension with phenyl lithium gave $[FeCp(CO)_2(phenyl)]$[5] while the reaction of $[FeCp(CO)(PPh_3)]Br$ with phenyl lithium afforded $[FeCp(CO)(PPh_3)(phenyl)]$. Replacement of one of the carbonyl ligands by a triphenylphosphine moiety was performed in order to stabilize the incipient carbon-metal σ-bond.

The $[1,4\text{-}\{FeCp(CO)_2\}_2(\mu\text{-phenylene})]$ complex was studied experimentally and theoretically with respect to delocalization effects. After using Fenske-Hall calculations on this disubstituted phenylene complex as well as several other organic models, Richardson and Hall[6] questioned the claims made by Hunter *et al*[7] regarding delocalization through a quinoidal bridge, which he based on spectroscopic evidence. They asserted that π-delocalization effects are unimportant in this compound. Sponsler[8] reported an in-depth theoretical study of delocalization effects on metal centres connected by conjugated bridges. Several diiron[9] and dirhenium[10] complexes with different conjugated systems were investigated.

Derivatives of five-membered heterocycles in which transition metals are connected to the α-carbons of the heterocyclic ring, have not received much attention in literature. Few of these complexes contain more than one metal fragment directly bonded to the heteroaromatic ring system. A small number of σ-2-furyl complexes is known in the literature compared to (2-thienyl)metal complexes, which are more abundant because of their relevance as model compounds for desulfurization processes. Typical examples of σ-2-furyl complexes are

---

[5] K.R. Aris, J.M. Brown, K.A. Taylor, *J. Chem. Soc., Dalton Trans.*, **1974**, 2222.

[6] N.A. Richardson, M.B. Hall, *Organometallics*, 12, **1993**, 1338.

[7] G.B. Richter-Addo, A.D. Hunter, *Inorg. Chem.*, 28, **1989**, 4063.

[8] M.B. Sponsler, *Organometallics*, 14, **1995**, 1920.

[9] N. Le Narvor, C. Lapinte, *J. Chem. Soc., Chem. Commun.*, **1993**, 357.

[10] Y. Zhou, J.W. Seyler, W. Weng, A.M. Arif, J.A. Gladysz, *J. Am. Chem. Soc.*, 115, **1993**, 8509.

[Au(PPh$_3$)2-furyl(CH$_3$)$_2$], [Pt(cod)(2-furyl)$_2$], [Pt(cod)Cl(2-furyl)][11] and [ZrCp$_2$(2-furyl)$_2$][12]. Onitsuka *et al*[13] prepared [Pt(PBu$_3$)$_2$(2-thienyl)$_2$] as well as 2,5-thienylene-bridged diplatinum complexes and found that these bimetallic complexes have d_π-p_π interaction between two platinum atoms through the thienylene bridge. They extended this study to include bithiophene as bridging ligand. The reactivity of these and similar complexes towards isocyanide were investigated[14], based on the unique reactivity of μ-ethynediyl complexes of palladium and platinum with isocyanide[15]. Synthesis of the 2-thienyl and 2,5-thienylene platinum compounds were accomplished *via* a 2-trimethylstannylthiophene[11c] and a 2,5-bis(trimethylstannyl)thiophene[16] precursor (figure 5.2). Nickel and palladium complexes were prepared in a similar fashion.

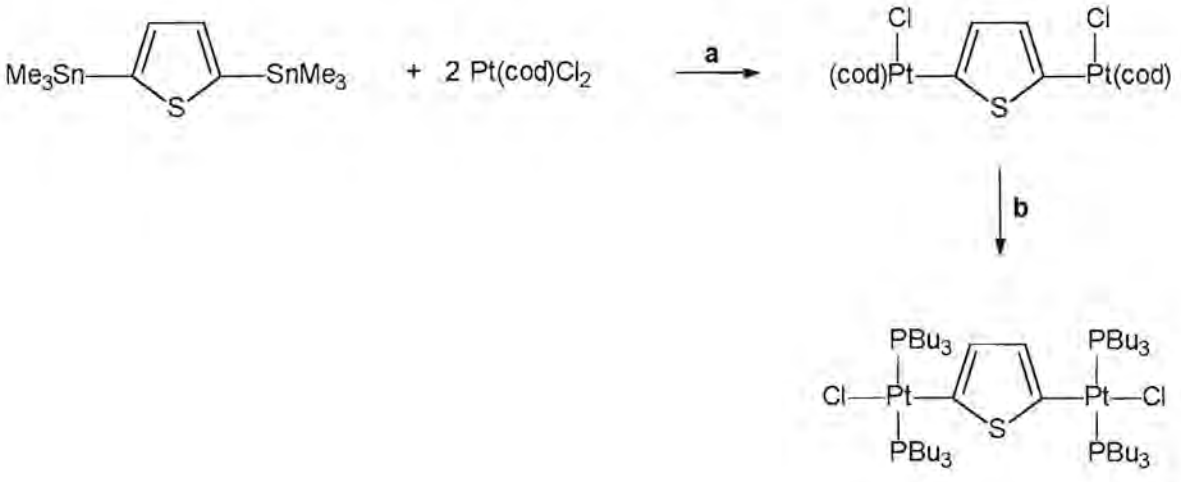

Figure 5.2 Synthesis of 2,5-thienylene diplatinum complexes
Reagents and conditions: (**a**) CH_2Cl_2, reflux 4 h; (**b**) 4PBu_3, CH_2Cl_2, RT, 4h

---

[11] (a) S. Komiya, S. Ozaki, A. Shibue, *J. Chem. Soc., Chem. Commun.*, **1986**, 1555. (b) C. Eaborn, K.J. Kevin, A. Pidcock, *J. Chem. Soc., Dalton Trans.*, **1978**, 357. (c) J. Müller, C. Friedrich, *J. Organomet. Chem.*, 377, **1989**, C27.

[12] G. Erker, R. Petrenz, C. Krüger, F. Lutz, A. Weiss, S. Werner, *Organometallics*, 11, **1992**, 1646.

[13] K. Onitsuka, K. Murakami, K. Matsukawa, K. Sonogashira, T. Adachi, T. Yoshida, *J. Organomet. Chem.*, 490, **1995**, 117.

[14] S. Kotani, K. Shiina, K. Sonogashira, *J. Organomet. Chem.*, 429, **1992**, 403.

[15] K. Onitsuka, T. Joh, S. Takahashi, *J. Organomet. Chem.*, 464, **1994**, 247.

[16] C. van Pham, R.S. Macomber, H.B. Mark, H. Zimmer, *J. Org. Chem.*, 49, **1984**, 5250.

These reactions were carried out according to the method employed by Müller and Brune[17] for the preparation of disubstituted phenyl platinum complexes. Evidence of metal-metal communication[18] through the conjugated ring system prompted further studies of thiophene and similar compounds. Upon treating the 2,5-thienylene diplatinum complexes with *p*-tolyl isocyanide at elevated temperatures, one molecule of isocyanide inserted into each Pt-C bond (figure 5.3)[13].

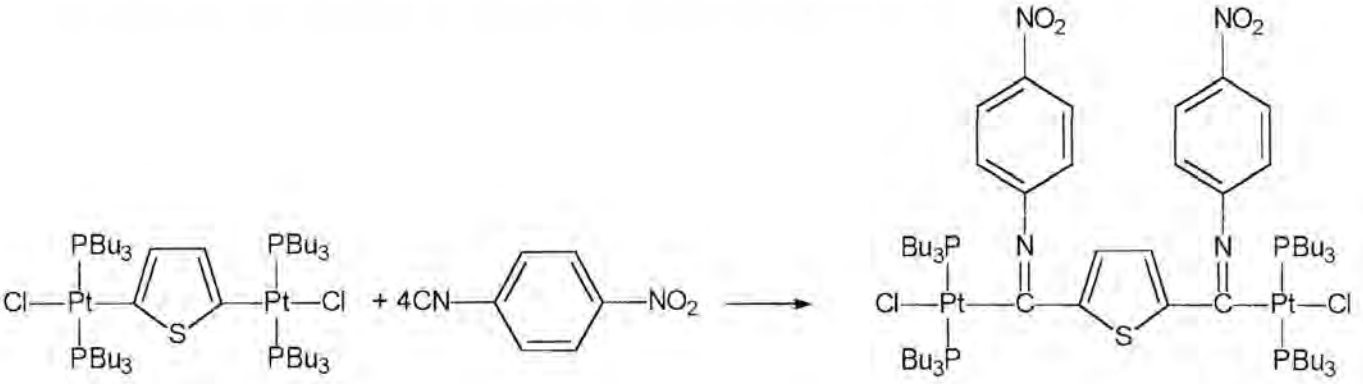

Figure 5.3 Reaction of 2,5-thienylene diplatinum complexes with isocyanide

Rauchfuss *et al*[19] embarked on the study of developing the chemistry of complexes with multiple thienyl ligands. Justification for this research was found in the rich chemistry of polyaryl metal complexes and it was suggested that, since thiophene is more reactive than benzene towards electrophiles and also more acidic, the polythienyl ligands should display novel reactivity. Known metallocene complexes of the type $[MCp_2(2\text{-thienyl})_2]$ include the transition metals Ti, Zr, Hf, Nb and W[20].

Angelici *et al*[21] synthesized $[ReCp(PPh_3)(NO)thiophene]^+$ to explore reactions of S-coordinated thiophenes, which undergo C-H cleavage to yield thienyl complexes. $[ReCp(PPh_3)(NO)thiophene]^+$ reacts with potassium hydroxide in methanol to afford $[ReCp(PPh_3)(NO)2\text{-thienyl}]$

---

[17] W.D. Müller, H.A. Brune, *Chem. Ber.*, 119, **1986**, 759.

[18] U. Bayer, H.A. Brune, *Z. Naturforsch., Teil B*, 38, **1983**, 632.

[19] P.R. Stafford, T.B. Rauchfuss, S.R. Wilson, *Inorg. Chem.*, 34, **1995**, 5220.

[20] V.A. Knizhnikov, Yu.A. Ol'dekop, *J. Gen. Chem. USSR (Engl. Transl.)*, 55, **1985**, 1385.

[21] M.J. Robertson, C.J. White, R.J. Angelici, *J. Am. Chem. Soc.*, 116, **1994**, 5190.

Silylthiophenes have recently received considerable attention due to several reasons. Firstly they have been recognized as starting materials for the preparation of polythiophenes[22]. Furthermore, the presence of a trimethylsilyl group on the 2-position serves as a protecting group towards metallation[23] directed at the 3-position specifically. 2-Trimethylsilylthiophene was synthesized by Deans and Eaborn[24], while the 2,5-bis(trimethylsilyl)thiophene was prepared by Sauvajol (65% yield)[25] as well as by Van Pham (89% yield)[16] but by using different silylation methods. Both complexes were synthesized *via* the appropriate bromothiophene precursor. Although many studies of polycarbosilanes have appeared in literature, their germanium backbone analogues have been neglected until recently. The polymer [2,5-(dimethylgermyl)thiophene]$_n$ was prepared by Barrau *et al*[26] by poly-condensation between 2,5-dilithiothiophene and dichlorodimethylgermanium (80% yield). The formation of [2,5-bis(chlorodimethylgermyl)thiophene] (20% yield) was also observed in the same reaction.

Nesmeyanov and co-workers reported the syntheses of σ-complexes of manganese pentacarbonyl with furan, benzofuran and thiophene[27]. The monosubstituted σ-complexes of perchlorothiophene with nickel, iron and manganese derivatives have also been synthesized previously[28]. Iron complexes of the type [FeCp(CO)$_2$R], with R = 2-thienyl, 2-furyl, 5-methyl-2-furyl and 4,5-benzo-2-furyl were synthesized by the initial reaction of Na[FeCp(CO)$_2$] with 2-thiophenecarbonyl chloride (in the case of the thiophene product), followed by photochemical decarbonylation of these acyl complexes to yield the target products[29] (figure 5.4).

---

[22] H. Masuda, Y. Taniki, K. Kaeriyama, *Synth. Met.*, 55, **1993**, 1246.

[23] D. Häbich, F. Effenberger, *Synthesis*, **1979**, 841.

[24] F.B. Deans, C. Eaborn, *J. Chem. Soc.*, **1959**, 2903.

[25] J.L. Sauvajol, C. Chorro, J.P. Lère-Porte, R.J.P. Corriu, J.J.E. Moreau, P. Thépot, M. Wong Chi Man, *Synth Met.*, 62, **1994**, 233.

[26] J. Barrau, G. Rima, A. Akkari, J. Satge, *Inorg. Chim. Acta*, 260, **1997**, 11.

[27] A.N. Nesmeyanov, K.N. Anisimov, N.E. Kolobova, *Izv. Akad. Nauk SSSR, Ser. Khim.*, 1356, **1964**, 2247.

[28] M.D. Rauch, T.R. Criswell, A.K. Ignatovicz, *J. Organomet. Chem.*, 13, **1968**, 419.

[29] A.N. Nesmeyanov, N.E. Kolobova, L.V. Goncharenko, K.N. Anisimov, *Izv. Akad. Nauk SSSR, Ser. Khim.*, 1, **1976**, 153.

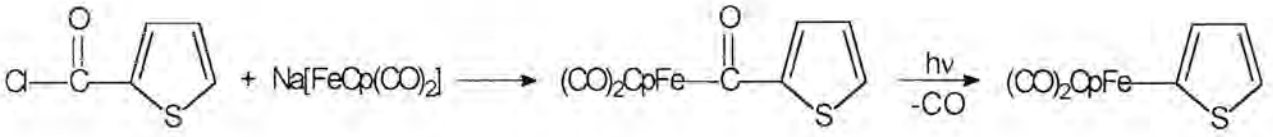

Figure 5.4 Synthesis of σ-iron heterocyclic complexes

Rauchfuss *et al*[30] prepared this same [$FeCp(CO)_2$(2-thienyl)] complex and studied its reaction with $Fe_3(CO)_{12}$. The expected thiaferrole complex was obtained, whereby an unusual synthetic route to multimetallic compounds is represented. This study was conducted in connection with research done on the activation and desulfurization of thiophene and benzothiophene by iron carbonyls.

2. Synthesis of iron complexes of Thiophene

The synthesis of iron complexes incorporating thiophene and derivatives thereof as bridging ligands was contemplated. Several different synthetic routes were explored and employed to try and synthesize these target molecules. The study was then to be extended to include other transition metals, for instance molybdenum, employing the most successful procedure for the syntheses of these complexes.

The first synthetic route employed was the synthesis *via* a dilithio intermediate, a similar method used by Lapinte *et al*[31] in synthesizing compounds consisting of long carbon chains capped with $FeCp(CO)_2$-metal moieties. The thiophene ligand was dilithiated using n-butyl lithium and TMEDA in a hexane solution at elevated temperatures. Upon reaction of 2,5-dilitiothienylene with $FeCp(CO)_2I$, two products were isolate, firstly the yellow mono [$FeCp(CO)_2$(2-thienyl] complex, previously prepared by Nesmeyanov *et al*[29], and secondly the orange coloured [2,5-{$FeCp(CO)_2$}$_2$thienylene] complex, **31**. This product was documented in a review article[32] but to

[30] A.E. Ogilvy, M. Draganjac, T.B. Rauchfuss, S.R. Wilson, *Organometallics*, 7, **1988**, 1171.

[31] F. Coat, C. Lapinte, *Organometallics*, 15, **1996**, 477.

[32] T.B. Rauchfuss, *Prog. Inorg. Chem.*, 39, **1991**, 259.

our knowledge the data has not yet been published. The structure of this complex is shown in the paper but until now not recorded in the Cambridge database. No details of the synthesis was given. Both the mono- and the bis complexes were formed in low yields.

The analogous reaction using 3,6-dimethylthieno[3,2-b]thiophene instead of thiophene, afforded four products (figure 5.5).

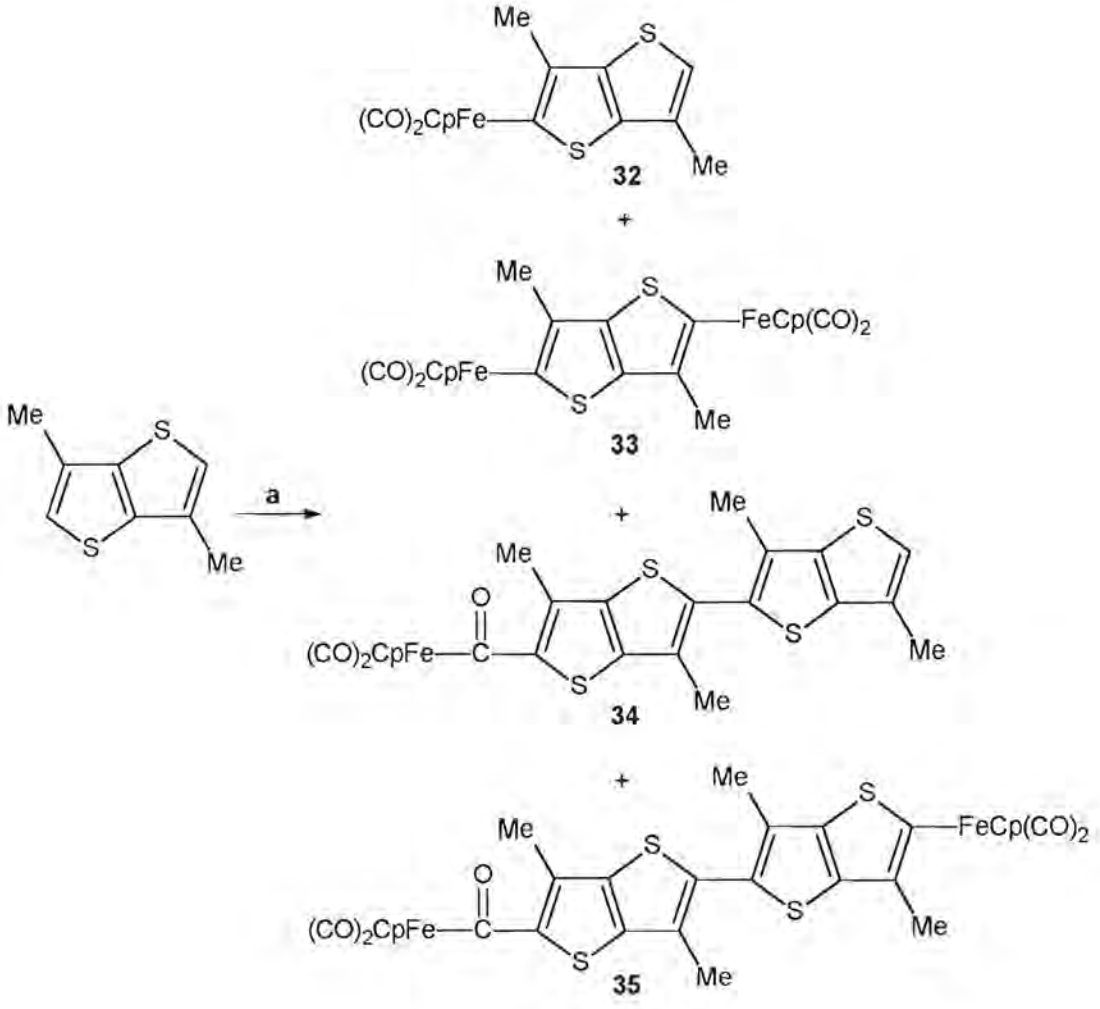

Figure 5.5 Synthesis of complexes **32-35**
Reagents: **a**(i) 2 eq. n-BuLi (ii) $FeCp(CO)_2I$

Again the mono-iron complex, **32**, as well as the bis complex, **33**, were formed, but the formation of two more products, complexes **34** and **35**, in which C-C coupling reactions are involved, is also

observed. The suggested mechanism for the formation of these two products is outlined in figure 5.6. The bis complex **33** is unstable and very reactive and we therefore conclude that it facilitated the formation of complexes **34** and **35**. It comprises the reaction of a diiron complex **33** and a mono-iron complex **32** to form complex **34** and the reaction between two bis-iron complexes **33** to form complex **35**. These reactions are thermodynamically favoured by the formation of the iron dimer [{FeCp(CO)$_2$}$_2$]. The insertion of a carbonyl group stabilizes the Fe-thienyl bond and thus the molecule. This proposed mechanism is supported by the presence of the dimer [{FeCp(CO)$_2$}$_2$] in the final reaction mixture. The same observation regarding the stability of these complexes were made as for the thiophene analogues. This reaction was also performed using the metal complex [MoCp(CO)$_2$Cl], but no organometallic products were formed during the reaction.

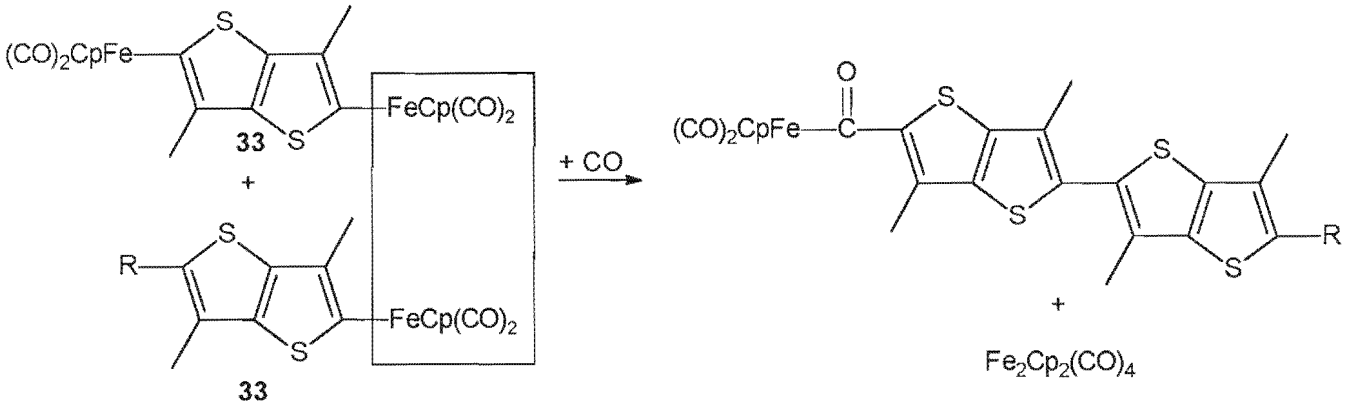

R = H **34**

R = FeCp(CO)$_2$ **35**

Figure 5.6 Reaction route for the formation of complexes **34** and **35**

It was obvious from the yields of the reaction products that these reactions had not gone to completion. It was suggested that the reason for the low reactivity between the two reagents could be ascribed to the relative strength of the Fe-I bond. By substituting the iodine ligand for a more labile leaving group on the metal, a higher yield of target products was envisaged. Therefore it was contemplated to repeat the reactions, but instead of reacting the lithio species with [FeCp(CO)$_2$I], [FeCp(CO)$_2$(O$_3$SCF$_3$)] was used, containing a triflate leaving group. This method, however, proved to be unsuccessful since only the mono-iron complex was obtained for both ligands.

The iron complex $Na[FeCp(CO)_2]$, prepared[33] from sodium amalgam and $[\{FeCp(CO)_2\}_2]$, was reacted with 2,5-dibromothiophene and 2,7-dibromo-3,6-dimethylthieno[3,2-*b*]thiophene, respectively, at -78°C. This preparation method was successfully employed by Hunter *et al*[4] for the syntheses of iron complexes with N-heterocycles. Unfortunately the target products were not afforded but only the starting materials were reclaimed. The same observation was made on repeating this reaction with $Na[MoCp(CO)_2]$.

In an attempt to stabilize the bis-iron complexes prepared *via* the lithio precursors, a test reaction was performed on the mono-iron complex **32**. Tertiary phosphine ligands are known to be strong donors of electronic charge and thus triphenylphosphine was chosen as a suitable ligand in substituting a carbonyl group. It was anticipated that the phosphine ligand would strengthen the iron-thienyl bond. A mixture of complex **32** and triphenylphosphine in hexane/ether (1:1) was irradiated for 30 minutes at 20°C. Only decomposition occurred and no evidence for the formation of a phosphine complex was observed.

Since the stability of the target products was one of the primary issues, the modification of the metal starting material $[FeCp(CO)_2I]$ was proposed. By incorporating the triphenylphosphine ligand into this metal complex and then reacting it with the lithio species, an enhanced stability of the products was foreseen. The reaction was effected similar to the reaction with $[FeCp(CO)_2I]$, but in this case no reaction product was isolated. This was again attributed to the relative strength of the Fe-I bond.

A new approach towards the synthesis of disubstituted iron complexes of thiophene derivatives was decided on, based on literature reports by Lo Sterzo *et al*[34]. They recounted the preparation of σ-metallaacetylides by palladium-catalyzed formation of metal-carbon bonds. The general procedure constitutes the coupling of halogen-containing transition metal moieties to mono- and bis[(trimethylstannyl)acetylides] in the presence of catalytic amounts of palladium. The 2,5-bis(trimethylstannyl)thiophene and the novel 2,7-bis(trimethylstannyl)-3,6-dimethylthieno[3,2-b]thiophene (complex **37**) were prepared in order to apply this method to our ligand systems.

---

[33] A.D. Hunter, A.B. Szigety, *Organometallics*, 8, **1989**, 2670.

[34] E. Viola, C. Lo Sterzo, F. Trezzi, *Organometallics*, 15, **1996**, 4352.

Complex **36**, the mono 2-(trimethylstannyl)-3,6-dimethylthieno[3,2-*b*]thiophene complex, formed as a byproduct in the preparation reaction of complex **37**. The planned synthetic route for preparation of the iron complexes is outlined in figure 5.7.

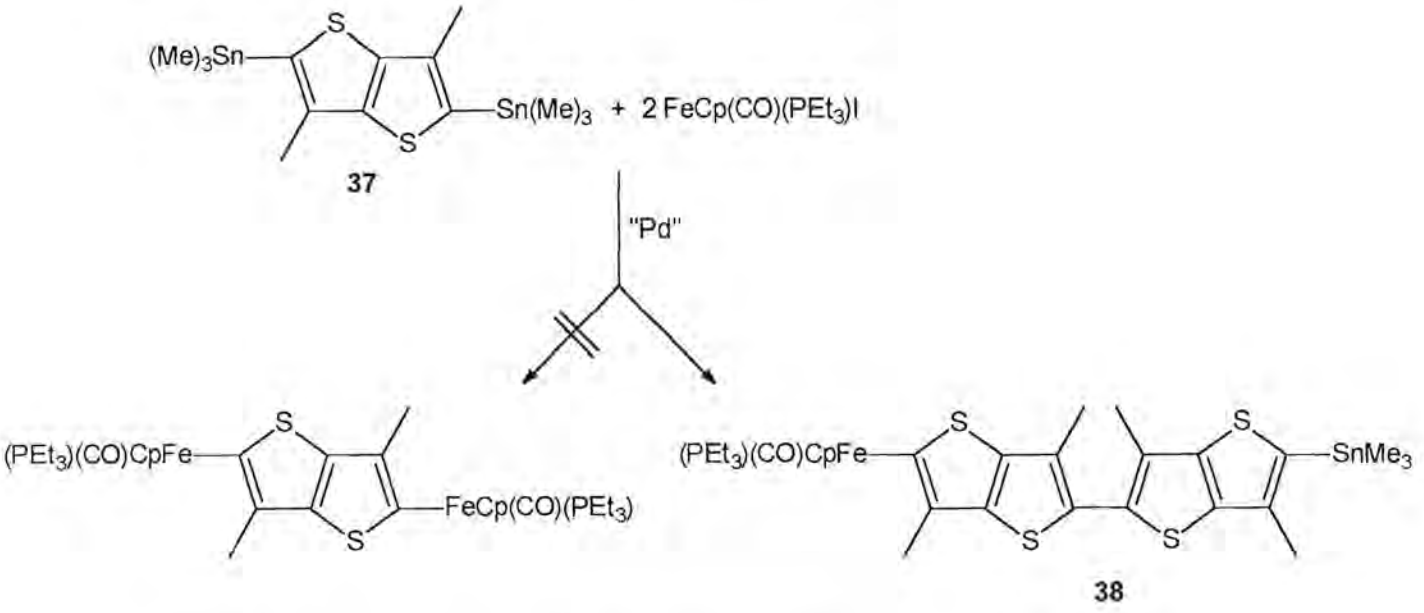

Figure 5.7 Proposed preparation of diiron complexes

After completion of the reactions for both ligands, it was only possible to isolate and characterize one product, complex **38**, formed in the reaction of $[FeCp(CO)_2I]$ with 2,7-bis(trimethylstannyl)-3,6-dimethylthieno[3,2-*b*]thiophene (complex **37**). This product was formed similar to the formation of complexes **34** and **35** and by the substitution of one of the trimethylstannyl groups by an iron metal fragment. Other products were also observed, but unfortunately their yields were too low to be able to isolate and characterize.

2.1 Spectroscopic characterization of novel complexes

The new iron complexes of the thiophene derivatives were characterized using ^{1}H NMR, ^{13}C NMR, infrared spectroscopy and mass spectrometry. Unfortunately many of the compounds were highly unstable and unsatisfactory ^{13}C NMR data were obtained due to decomposition. It was interesting to note that the thiophene complexes were seemingly more stable than their 3,6-dimethylthieno[3,2-*b*]thiophene counterparts, which is contrary to the trend observed for the

carbene complexes where the complexes with the condensed rings were more stable than the analogous thiophene complexes. Pauson suggested that the Fe-C_{arene} bond is stabilized by the effect of the condensed ring[35]. This same trend was observed by Nesmeyanov *et al*[29], who observed the stability of the [$FeCp(CO)_2$(2-benzofuryl)] complex compared to the iron complexes containing five-membered heterocyclic ligands.

2.1.1 ^{1}H NMR spectroscopy

All NMR spectra were recorded in deuterated chloroform as solvent unless otherwise specified. The ^{1}H NMR data for complexes **31-33** are summarized in table 5.1, while table 5.2 contains the data of complexes **34** and **35**. The data of complexes **36-38** are reported in table 5.3.

Table 5.1 ^{1}H NMR data of complexes 31, 32 and 33

Proton	Chemical shifts (δ, ppm) and Coupling constants (J, Hz)					
	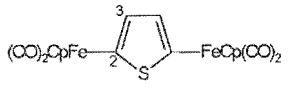 **31**		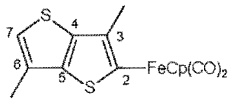 **32**		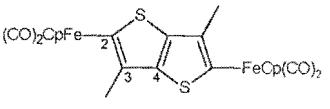 **33**	
	δ	J	δ	J	δ	J
H3	6.83 (s)	-	-	-	-	-
H4	6.83 (s)	-	-	-	-	-
H7	-	-	6.68 (q)	1.0	-	-
Me3	-	-	2.31 (s)	-	2.25 (s)	-
Me6	-	-	2.27 (d)	1.0	2.25 (s)	-
Cp	4.95 (s)	-	5.01 (s)	-	4.95 (s)	-

From the peaks observed on the spectra of the three complexes it is clear that ^{1}H NMR spectroscopy does not provide exclusive means for the characterization of these products. The protons observed do, however, indicate that both the metal fragment as well as the ligand are present in all of the complexes. The data for [$FeCp(CO)_2$(2-thienyl]][29] were found to be: 6.59 ppm

[35] P.L. Pauson, A.R. Quazi, B.W. Rockett, *J. Organomet. Chem.*, 7, **1967**, 325.

(H3), 6.84 ppm (H4), 7.18 ppm (H5) and 4.86 ppm (Cp).

The position of the Cp-ring on all three spectra is very similar although a more downfield shift is observed in the case of the mono-iron complex **32**. For this complex a quartet splitting pattern is found for the proton on the 7-position. This is due to long-range coupling with the methyl protons on the 6-position. For this methyl group a doublet is then also observed, instead of the expected singlet and the coupling constant of 1.0 Hz is calculated, correlating well with other four-bond couplings observed in literature[36].

Table 5.2 **^{1}H NMR data of complexes 34 and 35**

Proton	Chemical shifts (δ, ppm)	
	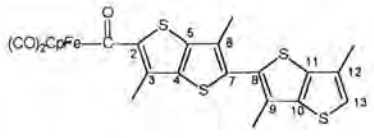 **34**	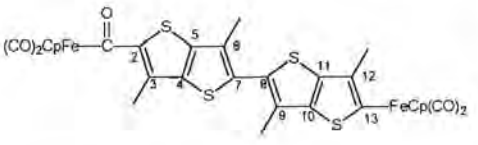 **35**
	δ	δ
H13	7.13 (s)	-
Me3	2.55 (s)	2.52[a] (br, s)
Me6	2.54 (s)	2.52 (br, s)
Me9	2.36 (s)	2.34 (br, s)
Me12	2.33 (s)	2.34 (br, s)
Cp	5.00 (s)	5.02 (br, s)

[a] Overlap of signals occur, broad bands observed

The spectra of the two complexes are, as expected, very similar. The methyl protons are little affected by changing form a mono complex to a dinuclear complex, since their values are very comparable for the two complexes. The spectrum of complex **35** is, however, affected by the coordination of a second metal moiety in that broad, undefined peaks are observed compared to the high resolution of the mono-nuclear complex. Interesting to note is the stability of the complex

[36] M. Hesse, H. Meier, B. Zeeh, *Spektroskopische Metoden in der organische Chemie*, Georg Thieme Verlag, Stuttgart, **1984**.

even though the metal is directly bonded to the ring system and carbonyl insertion did not take place to stabilize this second metal moiety. Previously it was shown in our laboratories that this second metal alkyl bond is stabilized by a carbonyl group inserted into the metal alkyl bond on the other side of a conjugated spacer[37].

Table 5.3 ^{1}H NMR data of complexes 36, 37 and 38

Proton	Chemical shifts (δ, ppm) and Coupling constants (J, Hz)					
	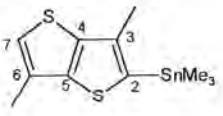 **36**		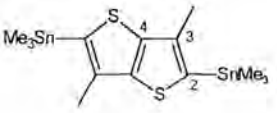 **37**		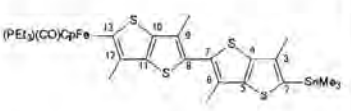 **38**	
	δ	J	δ	J	δ	J
H7	6.93 (s)	-	-	-	-	-
Me3	2.38 (s)	-	2.37 (s)	-	2.61 (s)	-
Me6	2.34 (s)	-	-	-	2.57 (s)	-
Me9	-	-	-	-	2.36 (s)	-
Me12	-	-	-	-	2.32 (s)	-
$SnMe_3$	0.42 (d)	56.1	0.40 (d)	55.8	0.05 (d)	56.8
Cp	-	-	-	-	5.28 (s)	-
$P(CH_2CH_3)_3$	-	-	-	-	1.23 (m)	-
$P(CH_2CH_3)_3$	-	-	-	-	0.84 (t)	6.3

Doublets are encountered on the spectra of complexes **36**, **37** and **38** for the methyl protons of the trimethylstannyl groups. These doublets are ascribed to coupling of these protons with the tin nucleus. A large coupling constant is observed for this coupling, which corresponds well with literature values[38].

---

[37] T.A. Waldbach, P.H. van Rooyen, S. Lotz, *Organometallics*, 12, **1993**, 4250.

[38] H. Friebolin, *Basic One- and Two-Dimensional NMR Spectroscopy*, VCH Verlag, Weinheim, **1993**, p.104.

2.1.2 ^{13}C NMR spectroscopy

The ^{13}C NMR data of complexes **31**, **32**, **34**, **36** and **37** are given in table 5.4.

Table 5.4 ^{13}C NMR data of complexes 31, 32, 34, 36 and 37

Carbon	Chemical shifts (δ, ppm)				
	31	**32**	**34**	**36**	**37**
	δ	δ	δ	δ	δ
C2	150.0	145.8	n.o.	145.4	147.6
C3	140.7	142.8	136.7	136.8	136.5
C4	140.7	n.o.	n.o.	142.4	134.9
C5	150.0	n.o.	n.o.	134.7	134.9
C6	-	136.3	135.9	122.1	136.5
C7	-	129.6	n.o.	130.1	147.6
C9	-	-	132.1	-	-
C12	-	-	125.3	-	-
C13	-	-	130.4	-	-
Me3	-	17.3	17.3	16.3	16.4
Me6	-	14.8	15.7	14.7	16.4
Me9	-	-	15.2	-	-
Me12	-	-	14.6	-	-
Cp	85.5	85.8	85.9	-	-
$M(CO)_2$	215.2	214.4	213.9	-	-
$SnMe_3$	-	-	-	-8.25	-8.33

Recording of ^{13}C NMR spectra proved to be problematic since the complexes were unstable at room temperature and even more so in solution. Decomposition occurred in several cases and made the unambiguous assignment of resonance peaks impossible. The fact that nearly all the carbons in the structure of the complexes are quaternary carbons, made the situation even worse. For complexes **33**, **35** and **38** only the distinguishable chemical shift values will be reported. Resonance peaks (ppm) were observed on the spectrum of **33** as follows: 214.2 ($M(CO)_2$), 85.8

(Cp), 17.2 (Me3, Me6). The resonance peaks on the spectrum of complex **35** were found at the following chemical shift values (ppm): 213.7 ($M(CO)_2$), 85.7 (Cp), 17.4 (Me3), 14.7 (Me6), 14.1 (Me9), 15.6 (Me12).

2.1.3 Infrared Spectroscopy

The infrared data of complexes **31-35** and complex **38** are outlined in table 5.5. All the spectra were recorded in dichloromethane as solvent.

Table 5.5 Infrared data of complexes 31, 32, 33, 34, 35 and 38

Band	Stretching vibrational frequency (v_{CO}, cm^{-1})					
	31	**32**	**33**	**34**	**35**	**38**
$A_1^{(1)}$	2025	2026	2023	2029	2053, 2028	1941
$A_1^{(2)}$	1972	1974	1972	1978	2007, 1978	-
C=O	-	-	-	1655	1656	-

Two bands were observed for the $M(CO)_2$ moieties while the inserted carbonyl band was observed at a characteristic value of 1656 cm^{-1} for both products containing this group.

2.1.4 Mass spectrometry

The fragmentation patterns of complexes **31**, **32**, **34**, **35**, **36** and **37** are presented in table 5.6. The molecular ion peak was observed on all the spectra except for the spectrum of complex **35**. The fragmentation pattern of these iron complexes constitute the elimination of the carbonyl groups of the metal moiety, followed by the loss of the inserted carbonyl (if present) and the loss of the cyclopentadienyl ring.

Table 5.6 Fragmentation patterns of complexes 31, 32, 34, 35, 36 and 37

Complex	Fragment ions (I, %)
31	435.8 (50) M^+; 407.8 (44) M^+ - CO; 379.8 (98) M^+ - 2CO; 351.8 (20) M^+ - 3CO; 323.8 (96) M^+ - 4CO; 258.8 (56) M^+ - 4CO - Cp; 193.9 (19) M^+ - 4CO - 2Cp; 83.0 (26) M^+ - 4CO - 2Cp -2Fe
32	343.9 (42) M^+; 316.0 (14) M^+ - CO; 287.9 (100) M^+ - 2CO; 222.9 (7) M^+ - 2CO - Cp; 167.0 (33) M^+ - 2CO - Cp - Fe
34	538.2 (36) M^+; 510.2 (4) M^+ - CO; 482.1 (100) M^+ - 2CO; 454.1 (8) M^+ - 3CO; 389.1 (2) M^+ - 3CO - Cp
35	573.9 (9) M^+ - 5CO; 509.3 (22) M^+ - 5CO - Cp; 443.2 (70) M^+ - 5CO - 2Cp
36	333.5 (38) M^+; 317.5 (93) M^+ - Me; 302.4 (30) M^+ - 2Me; 287.3 (9) M^+ - 3Me; 169.0 (100) M^+ - 3Me - Sn
37	494.5 (45) M^+; 479.5 (100) M^+ - Me; 449.4 (25) M^+ - 3Me; 419.3 (11) M^+ - 5Me; 404.2 (6) M^+ - 6Me

The molecular ion peak is present on the spectra of all the complexes, except complex **35** where the highest peak has a m/z value of 539.9. This peak is associated with the fragment where loss of all five carbonyl groups has occurred.

2.1.5 X-ray Crystallography

A single crystal X-ray diffraction determination confirmed the structure of complex **37**. The crystals were afforded from a dichloromethane:hexane (1:1) solution. Complex **37** crystallized as colourless cubic crystals. Figure 5.8 represents a ball-and-stick plot of this structure. Selected bond lengths and angles are given in table 5.7.

The bond angles around the sp^2-hybridized C(1) carbon atom are distorted from the normal value of 120°. This is evident when considering the bond angles C(2)-C(1)-Sn and S(1)-C(1)-Sn of 130.3(3)°and 117.6(2)°, respectively. This phenomenon is attributed to the presence of the methyl substituents on the arene ring, causing steric interaction with the methyl groups of the metal fragment. The result is the deformation of the molecule where the metal moiety is bent towards the sulfur atom of the ring.

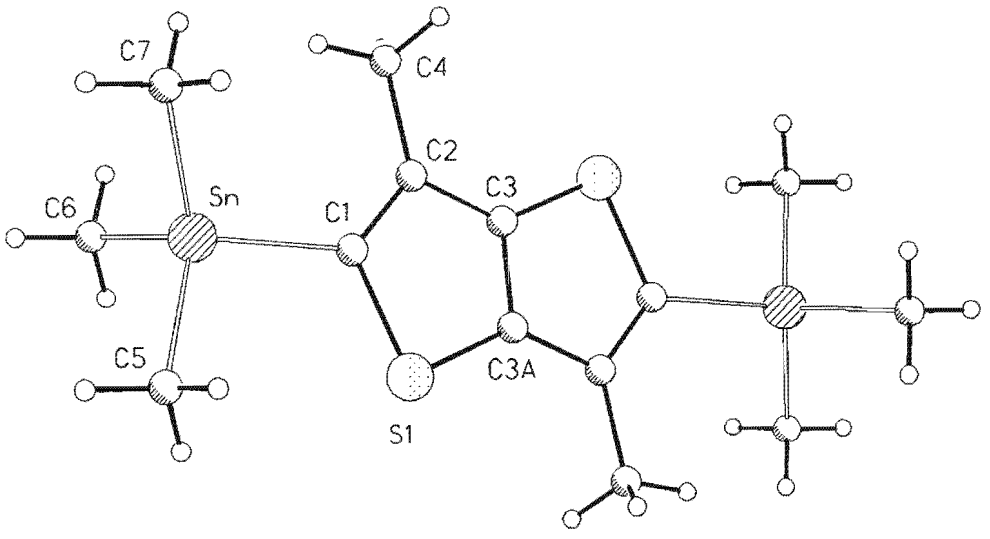

Figure 5.8 Ball-and-stick plot of complex **37**

Table 5.7 Selected bond lengths and angles of complex 37

37	Bond lengths (Å)	37	Bond angles (°)
Sn-C(1)	2.152(3)	C(3)#1-S(1)-C(1)	92.50(16)
S(1)-C(1)	1.757(3)	C(2)-C(1)-S(1)	111.8(2)
C(1)-C(2)	1.369(5)	C(1)-C(2)-C(3)	111.3(3)
C(2)-C(3)	1.438(5)	C(3)#1-C(3)-C(2)	114.7(4)
C(2)-C(4)	1.513(5)		
C(3)-C(3)#1	1.395(7)		
C(3)-S(1)#1	1.730(4)		

The metal moiety is pseudotetrahedral, evident from the bond angles around the tin atom the bond angles of C(7)-Sn-C(6) 109.9(2)°, C(7)-Sn-C(1) 112.4(2)°, C(6)-Sn-C(1) 107.0(1)°, C(7)-Sn-C(5) 110.1(2)°, C(6)-Sn-C(5) 111.4(2)° and C(1)-Sn-C(5) 105.9(2)° are marginally different from the normal value of 109° for tetrahedral arrangements. The Sn-C(thienyl) bond length is the same (2.15 (1) Å) as those recorded for the same bonds in $Sn(thienyl)_4$[39] and the 2.14 (1) Å recorded

[39] A. Karipides, A.T. Reed, D.A. Haller, F. Hayes, *Acta Cryst. B*, 33, **1977**, 950.

for the analogous Sn(phenyl)$_4$[40]. These distances are similar to the average bond length of 2.14 Å found for Sn-C(Me) bonds. The Sn-C(1) bond length of 2.152(3) Å can not be compared to Sn-C bond lengths of organotin halides. The Sn-C bond length in $SnMe_2F_2$[41] and $SnMe_2Cl_2$[42] is 2.08 Å and 2.21 Å respectively. The variation in Sn-C bond lengths can be correlated with the electronegativity and size of the halogens.

[40] V.K. Belsky, A.A. Simonenko, V.O. Reikhsfeld, L.E. Saratov, *J. Organomet. Chem.*, 244, **1983**, 125.

[41] E.O. Schlemper, *Inorg. Chem.*, 5, **1966**, 507, 511.

[42] A.G. Davies, *J. Chem. Soc. (A)*, **1970**, 2862.

6 Conclusion

1. General

The synthesis of binuclear complexes with conjugated spacer units was put forward as the first stage in preparing complexes specifically tailored for metal-metal communication and charge transfer for application in materials. The synthesis of stable binuclear complexes containing different end-capped metal moieties was envisaged as the eventual objective and can be seen as an extension of this study. The synthesis of the conjugated spacer units proved to be the more challenging part of the syntheses in this study, since the Fischer carbene method employed in the preparation of the novel carbene complexes has already been extensively studied and applied in literature. Metallation of the heteroaromatic substrates was readily accomplished and alkylation of the acyllated intermediate salts was effected effortlessly. Unfortunately the formation of byproducts such as the monocarbene complexes, due to incomplete metallation, and the decomposition products, due to the instability of the biscarbene complexes, influenced the yields of the binuclear complexes and thus the stability of these and similar complexes requires further investigation.

The stabilities of the novel complexes were not formally investigated, but the rates of decomposition of the different complexes in solution and on exposure to air were used as a criterion. It was found that the stability of the complexes increased on increasing the number of condensed thiophene fragments in the ring system. For instance, the molybdenum biscarbene complex of thiophene decomposed overnight in an inert atmosphere, stored below 0 °C, while the analogous biscarbene complex containing a dithienothiophene ligand was air-stable for two days before decomposing. For the iron complexes, the opposite trend was observed. Complexes containing thiophene units were more stable and accessible than thienothiophene analogues. The stability of the different metal complexes was found to follow the following trend: W > Cr > Mo.

2. Electronic spectra

Three intense bands are present on the UV-spectrum of thiophene in the gas phase, at 240 nm, 207 nm and 188 nm. Two bands, at 215 nm and 231 nm, are observed on the spectrum of thiophene in solution. Substituents on the ring have an influence on the position of these bands, depending on the ring position of the substituent. As the number of conjugated thiophene units increases[1], the maxima of the absorption bands shift to longer wavelengths and the intensity of the absorbance increases with the lengthening of the thiophene annelation. This trend was also observed for the elongation of a C≡C bridging ligand[2] as well as for oligothiophenes. On increasing the number of thiophene moieties from one to three, an energy difference of *ca.* 100 nm was observed[3]. Four bands can be distinguished on the spectrum of thieno[3,2-*b*]thiophene, at 253 nm, 261 nm, 270 nm and 280 nm. On the spectrum of dithieno[3,2-*b*:2',3'-*d*]thiophene three bands are distinguished at 282 nm, 292 nm and 304 nm.

The UV-spectra of a few of the novel complexes were recorded in dichloromethane. The electronic data of the series **22**, **23** and **24** and the series **13** and **27** are produced in table 6.1 and the electronic spectrum of complex **23** is presented in figure 6.1. All the complexes exhibit strong ligand-based absorption bands between 223 and 245 nm. Intense characteristic absorption bands with λ_{max} in the range 330 to 390 nm are assigned to the thiophene-based π-π* transitions. Coordination to metal fragments shift these bands to higher wavelengths, indicating interaction of the metal carbene π-system with that of the thiophene substituent. The energies of the π-π* transitions in the thiophene are reduced. For example, compare the bands in the range 282-304 nm for thienothiophene with a range of 320-388 nm observed for complex **23**. Also, bands are more intense in the spectra of the biscarbene complexes as the corresponding bands for the monocarbene complexes. The energy of the transition shifts to higher energy as the number of thienyl fragments in the complexes increases. This is demonstrated in going from **13** to **24** to **27**. The absorption band at lowest energy is assigned to a d-p metal-to-ligand charge transfer

---

[1] Y. Mazaki, K. Kobayashi, *Tetrahedron Lett.*, 30, **1989**, 3315.

[2] C. Hartbaum, E. Mauz, G. Roth, K. Weissenbach, H. Fischer, *Organometallics*, 18, **1999**, 2619.

[3] Y. Zhu, D.B. Millet, M.O. Wolf, S.J. Rettig, *Organometallics*, 18, **1999**, 1930.

transition. Since the colours of the different complexes are characteristic to the number of metal moieties coordinated to the ligand, it is not surprising that the values of this transition are very similar for the different types of complexes. Biscarbene complexes are all purple coloured for Cr, W and Mo complexes and purple-brown for Mn complexes and the absorption band is observed in the range 550 to 570 nm. This phenomenon also applies to the orange-red monocarbene complexes of Cr, W and Mo, with the absorption energy ranging from 460 to 493 nm in these complexes.

Table 6.1 UV data of complexes 13, 22, 23, 24 and 27

Complex	Colour	Ligand π-π* transition (λ, nm)	Metal-ligand transition (λ, nm)
22	Orange-red	373	493
23	Purple	340, 358	565
24	Orange-pink	358	505
13	Orange	349	463
27	Orange	373	490

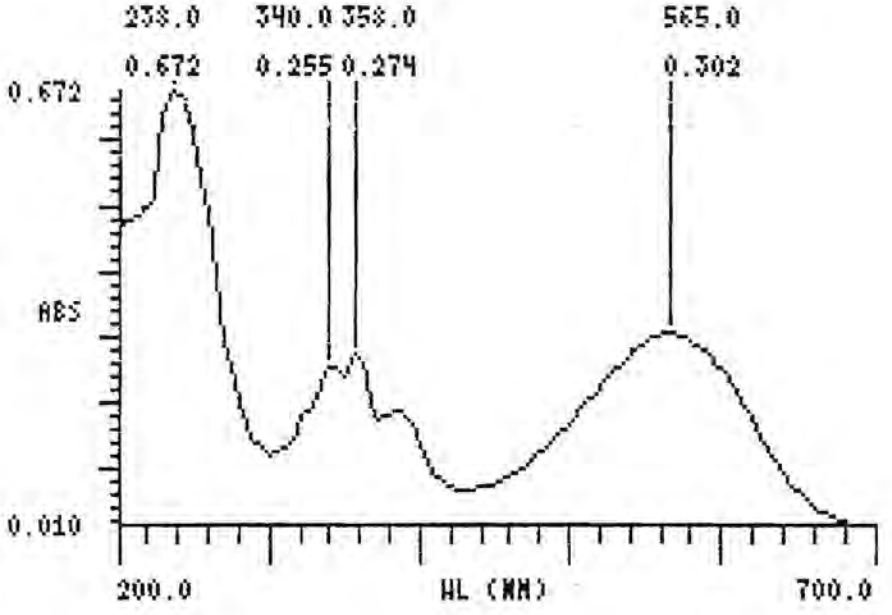

Figure 6.1 UV-spectrum of complex **23**

3. Structural features of the novel complexes

On scrutinizing the structural geometries of the complexes with thiophene, thienothiophene and dithienothiophene units, it seems as if the conformation where the metal fragment is positioned on the opposite side of the sulfur atom in the ring is preferred and a crab-like structure is observed for biscarbene complexes. This geometry was encountered for the structures of complexes **1**, **19**, **22**, **23** and **27**. The opposite conformation, where the metal fragment is directed towards the sulfur atom in the ring, was only found for complexes containing a 3,6-dimethyl[3,2-*b*]thiophene ligand, *i.e.* complexes **8**, **9**, **11**, **12**, **16** and **18**. It was suggested that steric influences of the methyl substituents on the ring prevented the positioning of the metal moiety on that side of the ligand.

On comparing the crystal data of all the different structures, it is evident that the heteroaromatic ligand is planar for all the complexes and it is thus possible to facilitate the delocalization of electron density through the π-system of the ligand. The torsion angles presented in table 6.2 confirm the planarity of the ring system, with small distortions observed for some of the complexes. These distortions are mostly observed in the structures of the biscarbene complexes and the decomposition products. The greatest deviation in the planarity of the ring itself is obtained for complex **19**, a decomposition product, with a value of 5.3°. In biscarbene complexes metal-metal communication through this delocalized system seems plausible.

For the monocarbene complexes **1**, **8** and **11** the metal atom, carbene carbon and arene ring are all exactly coplanar. In the case of the biscarbene complexes, distortion of the metal atom out of the carbene-arene plane ranges from 10° to 25°, with the greater deviations observed in complexes containing 3,6-dimethylthieno[3,2-*b*]thiophene. These distortions may be due to the position of the metal moiety on the same side as the sulfur atom in the ring, which is possibly not the preferred position of the metal fragment, as was suggested earlier. It is however forced into this orientation by the steric methyl substituents on the ring, occupying the space preferred by the metal moiety. The greatest deviation is again observed in complex **19**, where the metal is bent out of the plane at an angle of 31.2°.

Table 6.2 Magnitude of torsion angles in structures

Complex	Torsion angle (°)						
	M-C1-C2-S	M-C1-C2-C3	C1-C2-C3-C4	S1-C5-C4-S2	C3-C4-C5-C6	S2-C7-C6-S3	C5-C6-C7-C8
1	180.0	0.0	180.0	-	-	-	-
8	0.0	180.0	180.0	180.0	180.0	-	-
9	24.6	152.5	176.5	-	-	-	-
11	0.0	180.0	180.0	180.0	180.0	-	-
12	25.3	152.0	176.6	-	-	-	-
16	8.3	173.8	179.7	178.1	178.1	-	-
18	19.8	157.6	177.5	-	-	-	-
19	148.8	28.4	174.7	179.1	176.8	-	-
22	168.1	11.5	178.4	178.6	179.4	178.4	179.4
23	166.0	10.6	176.3	179.0	176.7	177.9	175.5
27	178.3	2.0	179.1	179.7	179.2	177.0	176.3

Further evidence for the delocalization of the electron density in the heteroaromatic ring can be found in the lengthening of the C-C bonds of the ring system. This phenomenon is more prominent for biscarbene complexes than for the monocarbene or decomposition products. In going from one (thiophene) to two (thienothiophene) to three (dithienothiophene) condensed thiophene rings, it is interesting to note that the ring directly coordinated to the carbene moiety is the most affected by the delocalization effect while the second and third thiophene units are less affected. Bond lengths for the other rings indicate more localized bonding which are also more comparable in length to those of the free thiophene. Contributing resonances are outlined in figure 6.2. From the resonance structures of the complexes in figure 6.2 it is evident that the delocalization effect of the electron density in the ring will influence the bond length of the C(2)-C(3) bond the most. This is confirmed on the structural data of all the complexes (table 6.3). It is interesting to note that this effect is more enhanced for the monocarbene complexes and the decomposition products. The average bond length for this bond in the structures of the three ring systems is 1.35 Å. The decrease in bond length of the C(3)-C(4) bond in the complexes compared to the free ligand is observed in only a few cases but these differences are too insignificant to fully justify the existence of this resonance structure.

Table 6.3 C(2)-C(3) bond distances

Complex	C(2)-C(3) bond (Å)	Complex	C(2)-C(3) bond (Å)
1	1.380(8)	**18**	1.394(7)
8	1.413(6)	**19**	1.384(4)
9	1.393(4)	**22**	1.401(9)
11	1.402(8)	**23**	1.396(11)
12	1.399(10)	**27**	1.400(11)
16	1.410(8)		

Thiophene:

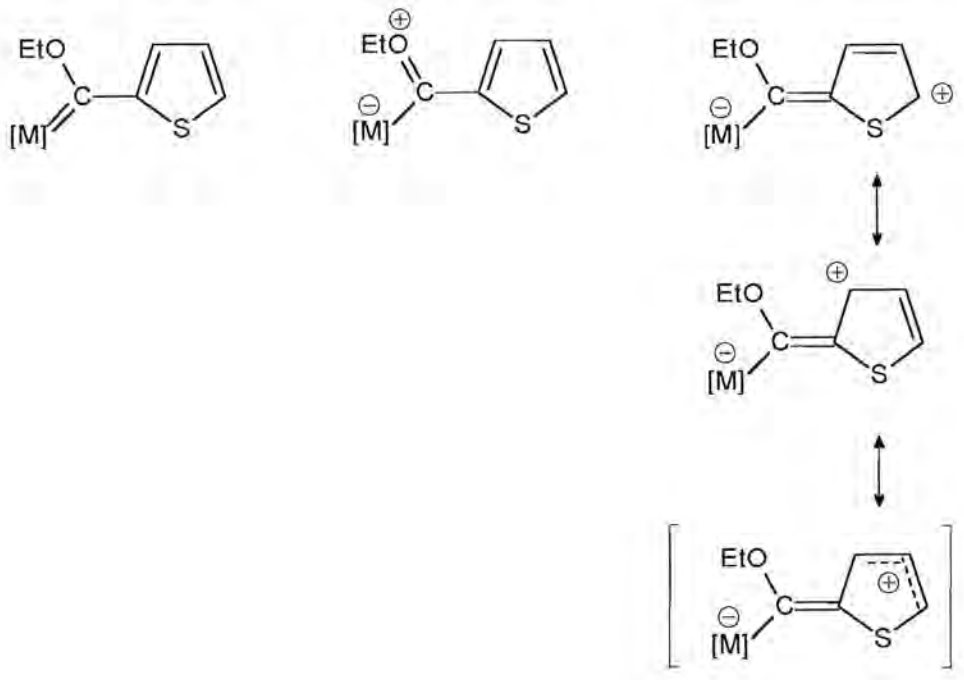

Thienothiophene:

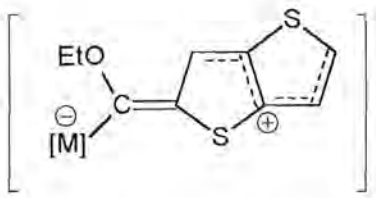

Dithienothiophene:

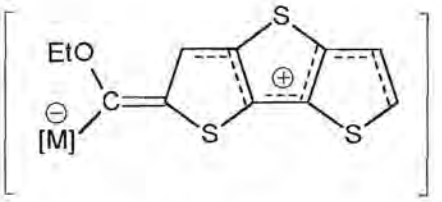

Figure 6.2 Resonance structures showing delocalization in thiophenes

In conclusion: It is possible to synthesize and fully characterize biscarbene complexes with condensed thiophene spacer units. Spectroscopic and structural features of this new complexes reveal thiophene involvement with the metal fragments *via* the carbene carbon atoms. Insight into the stability of the complexes on variation of the number of rings in the spacer is valuable information for future design and studies. Comparison with oligothiophene spacer units in similar complexes is a worthwhile expansion of this study and an in-depth investigation into the role of the sulfur atoms in the rings to enhance the charge transfer phenomenon along the chain is essential. These complexes represent a different variation of the "molecular wire" concept as it is now part of a band structure between two end poles. The unique features of activated sites in the new biscarbene complexes open various opportunities for novel syntheses in organic chemistry. Also, as a probe in well-known carbene reactions such as the Dötz and other reactions , it could afford interesting intermediates involving metallacycles which could aid in unraveling the mechanisms of these processes.

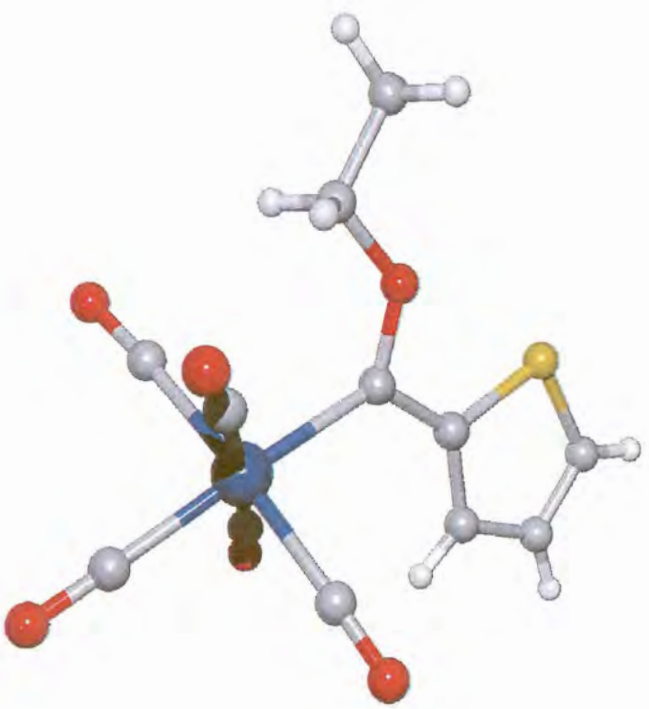

Figure 6.3 Crystal structure of complex **1**

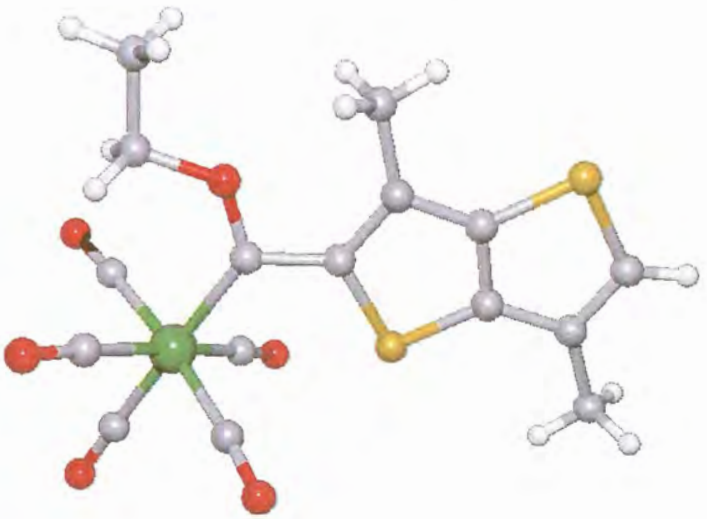

Figure 6.4 Crystal structure of complex **8**

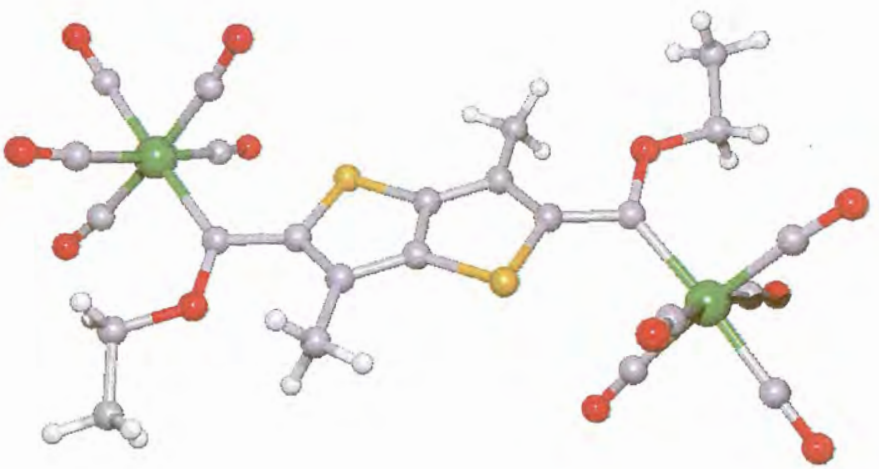

Figure 6.5 Crystal structure of complex **9**

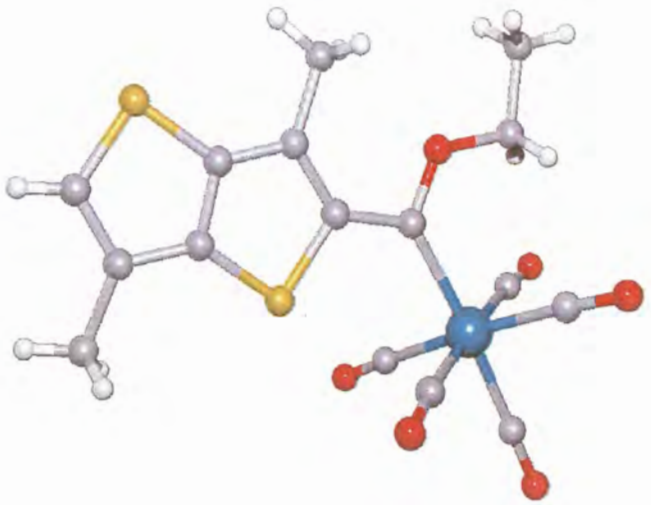

Figure 6.6 Crystal structure of complex **11**

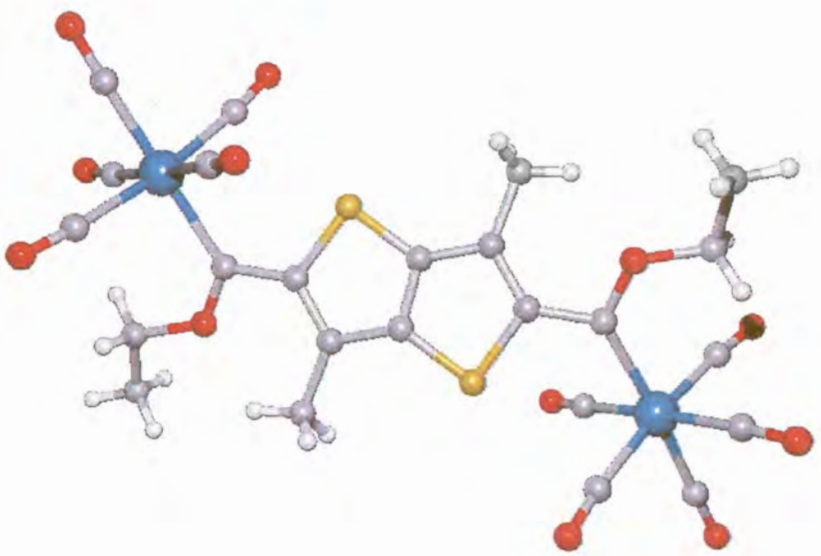

Figure 6.7 Crystal structure of complex **12**

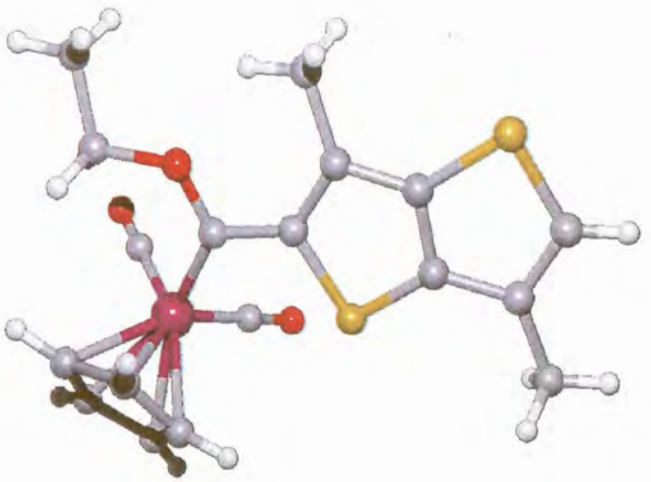

Figure 6.8 Crystal structure of complex **16**

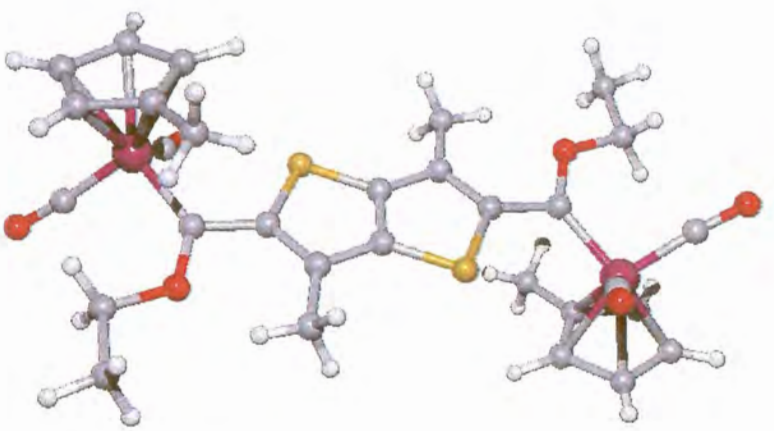

Figure 6.9 Crystal structure of complex **18**

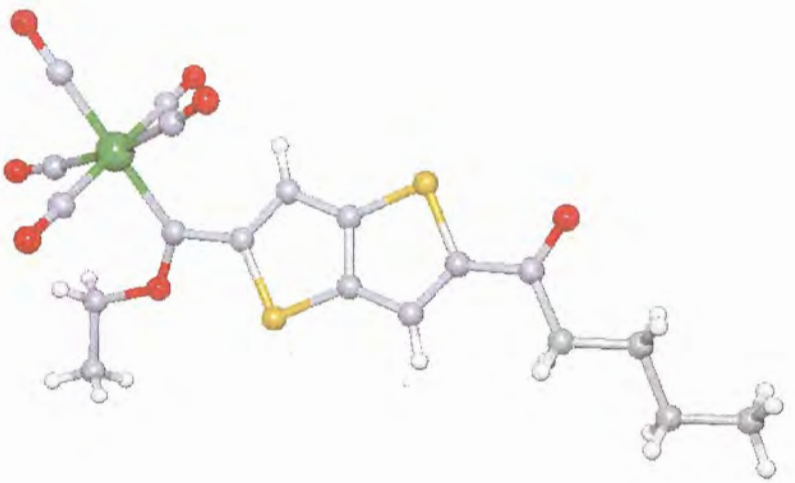

Figure 6.10 Crystal structure of complex **19**

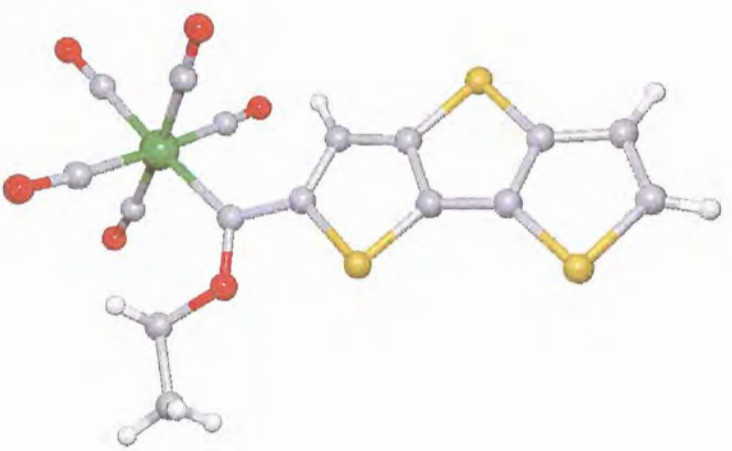

Figure 6.11 Crystal structure of complex **22**

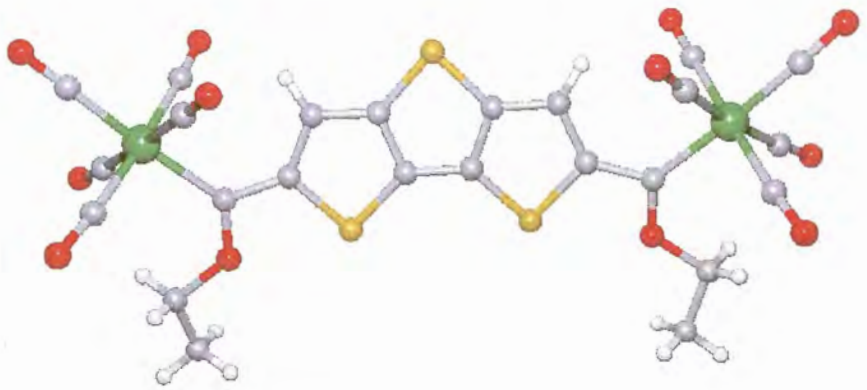

Figure 6.12 Crystal structure of complex **23**

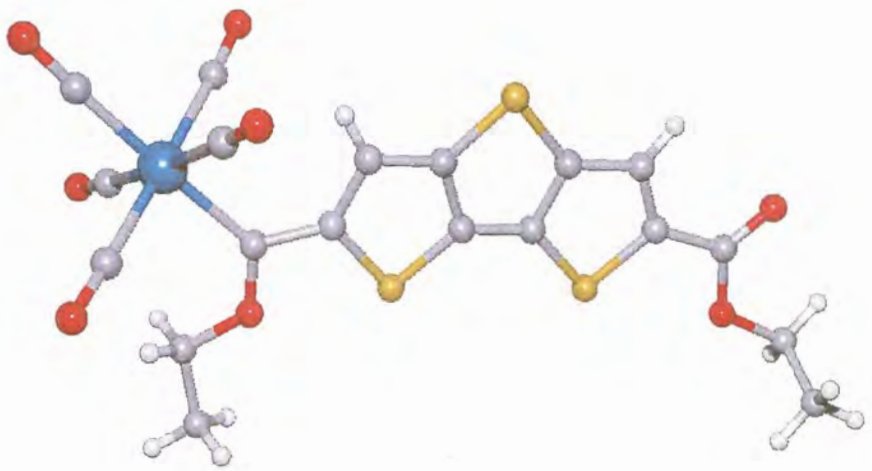

Figure 6.13 Crystal structure of complex **27**

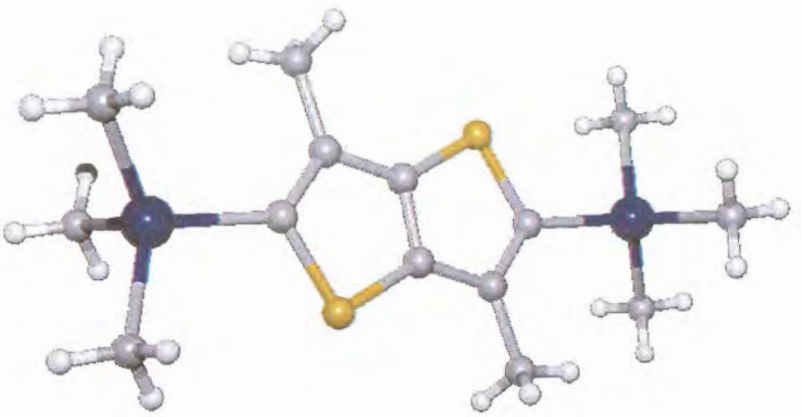

Figure 6.14 Crystal structure of complex **37**

7 Experimental

1. General

All reactions were performed in an inert atmosphere of either nitrogen or argon by using standard Schlenk techniques and vacuum-line. Solvents were dried and distilled under nitrogen prior to use. Column chromatography was carried out under nitrogen using either silica gel (particle size 0.063-0.200 nm) or neutral aluminium oxide as resin. Most chemicals were used directly without prior purification. Thiophene was purified as described by Spies and Angelici[1]. Trimethylamine N-oxide was azeotropically distilled from benzene and stored under argon.

1.1 Preparation of starting compounds

The following compounds were prepared using known literature methods: 3,6-Dimethylthieno[3,2-*b*]thiophene[2], 2,3,5-tribromothiophene[3], 3-bromothiophene[4], ethyl(3-thienothio)acetate[5], ethyl(2-formyl-3-thienothio)acetate[6], thieno[3,2-*b*]thiophene carboxylic acid, thieno[3,2-*b*]thiophene[4], cyclopentadienyliron dicarbonyl iodide[7], triethyl oxonium

---

[1] G.H. Spies, R.J. Angelici, *Organometallics*, 6, **1987**, 1902.

[2] K.S. Choi, K. Sawada, H. Dong, M. Hoshino, J. Nakayama, *Heterocycles*, 38, **1994**, 143.

[3] L. Brandsma, H.D. Verkruijsse, *Synthetic Comm.*, 18, **1988**, 1763.

[4] S. Gronowitz, T. Raznikiewicz, *Org. Synth. Coll.*, 5, **1973**, 149.

[5] Y.L. Goldfarb, V.P. Litvinov, S.A. Ozolin, *Izv. Akad. Nauk. SSR, Otd. Khim Nauk*, **1965**, 510.

[6] A. Bugge, *Chem. Scand.*, 22, **1968**, 66.

[7] R.B. King, F.G.A. Stone, *Inorg. Synth.*, 7, **1963**, 110.

tetrafluoroborate[8], 3,3'-dithienyl sulfide[9], 2,5-bis(trimethyltin)thiophene[10] and dithieno[3,2-*b*;2',3'-*d*]thiophene[11]. Cyclopentadienyliron triethylphosphino iodide was prepared by two separate syntheses. The first method[12] comprised the irradiation of cyclopentadienyliron dicarbonyl iodide in toluene in the presence of triethyl phosphine. The second synthesis was effected according to a method described by Moreno *et al*[13], using cyclopentadienyliron dicarbonyl iodide and trimethylamine N-oxide in THF in the presence of triethyl phosphine. It was concluded that the second preparation method afforded the highest yield of product.

1.2 Characterization of complexes

1.2.1 NMR spectroscopy

All NMR spectra were recorded in deuterated chloroform, unless stated otherwise, using the chloroform peak as standard on a Bruker ARX-300 spectrometer.

1.2.2 Infrared spectroscopy

Infrared spectra were recorded on a BOMEM FT-IR spectrophotometer using dichloromethane or hexane as solvent.

1.2.3. Mass spectrometry

Mass spectra were recorded at 70 eV on a Finnigan Mat 8200 instrument using the electron impact method.

---

[8] H. Meerwein, *Org. Synth.*, 46, **1966**, 113.

[9] L. Brandsma, H.D. Verkruijsse, *Preparative Polar Organometallic Chemistry 1*, Springer-Verlag, Berlin Heidelberg, **1987**, p.162.

[10] C. van Pham, R.S. Macomber, H.B. Mark, H. Zimmer, *J. Org. Chem.*, 49, **1984**, 5250.

[11] F. de Jong, M.J. Janssen, *J. Org. Chem.*, 36, **1971**, 1645.

[12] P.M. Treichel, D.A. Komar, *J. Organomet. Chem.*, 206, **1981**, 77.

[13] C. Moreno, M. Macazaga, R. Medina, D.H. Farrar and S. Delgado, *Organometallics*, 17, **1998**, 3733.

1.2.4 X-ray crystallography

Data collection and structure determinations were done by Dr. Helmar Görls, University of Jena, Germany. Experimental details for the X-ray analyses, listing of the experimental crystallographic parameters and tables of atomic coordinates, bond distances and angles, and anisotropic thermal parameters are available from the author on request.

2. Synthesis of Organometallic compounds

2.1 Thiophene carbene complexes

2.1.1 Synthesis of molybdenum complexes 1, 2, 3, 4 and 5

16.8 ml (26.8 mmole) of n-butyl lithium (15% solution in hexane) was added to a solution of 0.99 ml (12.4 mmole) of thiophene and 3.7 ml (24.7 mmole) of TMEDA in 50 ml of hexane at room temperature. The mixture was refluxed for 30 minutes during which time the lithium chloride salt precipitated as a white solid. This suspension was cooled to 0°C and 30 ml of THF was added. The mixture was then further cooled to -20°C and 5.99 g (22.7 mmole) of $Mo(CO)_6$ was added gradually. The reaction was kept at this temperature for 15 minutes, stirring vigorously, and then allowed to rise to room temperature. Stirring was continued for another hour, during which time the colour of the reaction mixture changed to a dark red-brown. After completion of the reaction, the solvent was evaporated *in vacuo*. 4.55 g (24.7 mmole) of triethyl oxonium tetrafluoroborate was dissolved in 20 ml of dichloromethane. This was added to the residue of the reaction mixture at -20°C and the solution, purple-coloured, was stirred for an hour while the temperature was allowed to rise to RT. The mixture was filtered through silica gel with dichloromethane and the solvent removed under reduced pressure. Column chromatography was used to purify the mixture of carbene products. Hexane was employed as starting eluent and the polarity was gradually increased by adding dichloromethane to separate the different compounds. Four compounds were isolated. The first yellow-orange product (yield: 1.53 g; 32%; mp.: 155°C dec.) was identified as the monocarbene complex **1**, while the second purple product (yield: 1.41; 17%) was characterized as the biscarbene complex **2**. This product decomposed with time to form the red decomposition product **3**, yield: 0.67 g (12%). The third product , also purple-coloured, was identified as complex **4**, yield: 2.08 g (20%). The last compound, isolated using pure

dichloromethane as eluent, was red and identified as complex **5**, yield:1.38 g (18%). The biscarbene complex **2** can be decomposed more rapidly on stirring in acetone or THF.

2.2 Aminolysis reactions of complex 1

2.2.1 Reaction with NH_3

0.55 g (1.5 mmole) of the molybdenum monocarbene complex **1** was dissolved in 50 ml of diethyl ether. Ammonia was bubbled through the solution for 5 hours. The solvent was removed under reduced pressure and the residue purified using column chromatography. Two bands were separated: unreacted starting complex **1** (yield: 0.23 g; 41%) and a yellow product **6**, (yield: 0.24 g; 46%).

2.2.2 Reaction with 1,4-phenylene diamine

0.55 g (1.5 mmole) of the molybdenum monocarbene complex **1** was dissolved in 50 ml of diethyl ether. A solution of 0.33 g (3.0 mmole) of 1,4-phenylene diamine in 10 ml of THF was added while stirring. The mixture was stirred for 24 hours. The solvent was removed under reduced pressure and the crude product purified on a silica column. Two bands were distinguished. The first yellow-orange band yielded the starting material **1**, (yield: 0.29 g; 51%). The second yellow product isolated was identified as the aminocarbene complex **7**, yield: 0.28 g (42%).

2.3. 3,6-Dimethylthieno[3,2-b]thiophene and Thieno[3,2-*b*]thiophene carbene complexes

2.3.1 Synthesis of chromium complexes 8, 9 and 10

0.67 g (4.0 mmole) of DMTT was dissolved in 50 ml of hexane. 1.2 ml (8.0 mmole) of TMEDA and 5.5 ml (8.8 mmole) of n-butyl lithium were added at room temperature. The mixture was refluxed for 45 minutes and then cooled to 0°C. Lithium chloride precipitated as a white solid. After the addition of 50 ml of THF, 1.76 g (8.0 mmole) of $Cr(CO)_6$ was added and the suspension stirred for an hour. The colour of the reaction changed to dark brown. After completion of the reaction, the solvent was removed *in vacuo*. 1.50 g (8.1 mmole) of triethyl

oxonium tetrafluoroborate was dissolved in 20 ml of dichloromethane and this was added to the cooled reaction residue (-20°C) in dichloromethane. Immediately the colour change to a purple solution was observed. Stirring was maintained for a further hour while the temperature was allowed to reach room temperature. The mixture was then filtered, the solvent removed and the remainder purified on a silica gel column. Three products were isolated. The first was the orange monocarbene complex **8**, yield: 0.55 g (33%), mp.:173.4 - 176.8°C. The second purple complex was identified as the biscarbene complex **9**, yield: 1.25 g (47%). The third red-orange compound was characterized as **10**, yield: 0.23 g (12%).

2.3.2 Synthesis of tungsten complexes 11, 12 and 13

0.34 g (2.0 mmole) of DMTT was dissolved in 30 ml of hexane. 2.8 ml (4.4 mmole) of n-butyl lithium and 0.6 ml (4.0 mmole) of TMEDA were added to this solution at room temperature. The same procedure was followed as for the chromium analogue with the addition of 1.4 g (4.0 mmole) of $W(CO)_6$. For alkylation 0.74 g (4.0 mmole) of triethyl oxonium tetrafluoroborate was used. On purification using column chromatography, three bands separated. The first monocarbene complex **11**, was isolated as an orange solid with a yield of 0.45 g (41%); mp.:187.2 - 189.4°C. The second purple band, the biscarbene complex **12**, had a yield of 0.67 g (36%) while the third red-orange band was identified as (**13**), yield: 0.11 g (9%).

2.3.3 Synthesis of molybdenum complexes 14 and 15

The dilithio species, prepared according to the method described in **2.3.1**, was treated with $Mo(CO)_6$ (1.1 g, 4.0 mmole) at -20°C. The reaction mixture was stirred for 2 hours, while the temperature gradually rose to RT. The solvent was removed *in vacuo*. 0.74 g (4.0 mmole) of triethyl oxonium tetrafluoroborate in 50 ml of dichloromethane was added to the reaction residue and an immediate colour change from orange to purple was observed. Column chromatography yielded two products. The first orange product was identified as the monocarbene complex **14**, yield: 0.34 g (37%) while the second purple complex was the biscarbene complex **15**, yield: 0.32 g (21%). Several other complexes, in very low yields, were formed in this reaction but it was impossible to isolate or purify them.

2.3.4 Synthesis of manganese complexes 16, 17 and 18

(i) $Mn(C_5H_5)(CO)_3$

The reaction was carried out according to the general method described in **2.3.1** with the addition of 5.5 ml (8.8 mmole) of n-butyl lithium and 1.2 ml (8.1 mmole) of TMEDA to a solution of 0.67 g (4.0 mmole) of DMTT in 50 ml of hexane. 1.63 g (8.0 mmole) of $Mn(C_5H_5)(CO)_3$ was added to the dimetallated species. The reaction was effected with the addition of 1.5 g (8.0 mmole) of triethyl oxonium tetrafluoroborate and the subsequent purification on a silica gel column. Two products were isolated: the first reddish-brown monocarbene complex **16** (yield: 0.43 g; 27%) and the second purple-brown biscarbene complex **17** (yield: 1.49 g; 59%).

(ii) $Mn(C_5H_4Me)(CO)_3$

The metallation of DMTT was performed according to the method described in **2.3.1**, using 0.67 g (4.0 mmole) of DMTT. 0.92 g (8.0 mmole) of $Mn(C_5H_4Me)(CO)_3$ was added to the dilithiated species and alkylation was done with 1.5 g (8.0 mmole) of triethyl oxonium tetrafluoroborate. Column chromatography yielded mainly the biscarbene complex **18**, yield: 1.64 g (62%).

2.3.5 Synthesis of chromium complexes 19 and 20

Thieno[3,2-*b*]thiophene (0.56 g, 4.0 mmole) was dissolved in 30 ml of hexane. THF (100 ml) was added together with 1.2 ml (8.0 mmole) of TMEDA and 5.5 ml (8.8 mmole) of n-butyllithium. The mixture was refluxed for 45 minutes and cooled to 0°C after which 100 ml of THF was added. 1.7 g (8.0 mmole) $Cr(CO)_6$ was introduced and the mixture was stirred for an hour at room temperature. The solvent was evaporated and 1.5 g (8.0 mmole) triethyl oxonium tetrafluoroborate, dissolved in 30 ml of dichloromethane, was added at -30°C. The mixture was stirred for 15 minutes in the cold and for a further 45 minutes at room temperature after which it was filtered and the solvent evaporated. The residue was column chromatographed with a hexane: dichloromethane (1:1) solution to yield two products. The first purple-pink product was identified as **19**, yield: 0.79 g, 42% . The second orange product was characterized as **20** with a yield of 0.34 g, 14%.

2.4. Dithieno[3,2-b: 2',3'-d]thiophene carbene complexes

2.4.1 Synthesis of tungsten complex 21

3,3'-Dithienyl sulfide (0.79 g; 4.0 mmole) was dissolved in 30 ml of hexane. 5.5 ml (8.8 mmole) of n-butyl lithium and 1.2 ml (8.0 mmole) of TMEDA were added to this solution at room temperature. After refluxing the mixture for 45 minutes, it was cooled to 0°C and 20 ml of THF was added. Tungsten hexacarbonyl (1.4 g, 4.0 mmole) was introduced at -20°C with vigorous stirring and this was continued for one hour while the temperature was allowed to reach room temperature. The solvent was evaporated *in vacuo* and the residue dissolved in 50 ml of dichloromethane. Alkylation was effected with triethyl oxonium tetrafluoroborate (1.5 g, 8.0 mmole), which was dissolved in 30 ml of dichloromethane and added at -20°C. Stirring was maintained for one hour , the mixture was filtered through silica gel and the solvent removed. The green product, complex **21**, was isolated using column chromatography, with a yield of 1.26 g (52%).

2.4.2 Synthesis of chromium complexes 22, 23 and 24

0.19 g (1.0 mmole) of DTT was dissolved in 30 ml of hexane. 1.4 ml (2.2 mmole) of n-butyl lithium and 0.3 ml (2.0 mmole) of TMEDA were added to this solution at room temperature. This mixture was refluxed for 45 minutes and then cooled to 0°C. Lithium chloride precipitated from the yellow solution as a white solid. 30 ml of THF was added and the suspension was cooled even further to -40°C. 0.44 g (2.0 mmole) of $Cr(CO)_6$ was added and the colour of the mixture turned to red-brown. The temperature of the reaction was allowed to rise to room temperature while the mixture was stirred vigorously. After an hour the solvent was removed *in vacuo* and a solution of 0.4 g (2.0 mmole) of triethyl oxonium tetrafluoroborate in 50 ml of dichloromethane was added to the cooled residue (-20°C). After the addition of the alkylating agent, as room temperature was reached, the colour changed to dark purple. The mixture was filtered, the solvent removed. Three products were isolated using column chromatography. The first orange product was characterized as the monocarbene complex **22**, yield: 0.15 g (32%); mp. 181.5 - 183.7°C, while the second blue-purple product was identified as the biscarbene complex **23**, yield: 0.27 g (39%). The third product had a red-purple colour and was characterized as the decomposition product **24**, yield: 0.11 g (22%).

2.4.3 Synthesis of tungsten complexes 25, 26 and 27

1.4 ml (2.2 mmole) of n-butyllithium and 0.3 ml (2.0 mmole) of TMEDA were added to a solution of 0.19 g (1.0 mmole) of DTT in 30 ml of hexane. The reaction was effected in the same manner as described for the chromium analogue in **2.4.2.** with the addition of 0.70 g (2 mmole) tungsten hexacarbonyl and subsequent alkylation with 0.4 g (2.0 mmole) triethyl oxonium tetrafluoroborate.

Three products were isolated with column chromatography. The first orange product was identified as the monocarbene complex **25**, yield: 0.24 g (42%). The second purple was the biscarbene complex **26** which was formed in a yield of 0.25 g (26%). The third product had an brown-orange colour and was characterized as the decomposition product **27**, yield: 0.19 g (30%).

2.4.4 Synthesis of molybdenum complexes 28, 29 and 30

0.19 g (1.0 mmole) of DTT was dissolved in 30 ml of hexane after which 1.4 ml (2.2 mmole) of n-butyllithium and 0.3 ml (2.0 mmole) were added. The same reaction procedure was followed as described in **2.4.2** for the dilithiation of DTT. The addition of 0.53 g (2.0 mmole) of $Mo(CO)_6$ led to a dark brown colour change of the reaction mixture. Quenching the reaction with 0.4 g (2.0 mmole) triethyl oxonium tetrafluoroborate resulted in a purple-pink colour for the final reaction solution. Three products were purified on a column and isolated in the following order: the orange monocarbene complex **28**, yield: 0.13 g (26%); the purple biscarbene complex **29**, yield: 0.27 g (35%) and the pink-purple complex **30**, yield: 0.34 g (31%).

2.5. Alkyl complexes of Thiophene derivatives

2.5.1 Synthesis of iron complex 31

Dilithiation of thiophene was accomplished by adding 17.0 ml (27.3 mmole) of n-butyllithium and 3.7 ml (24.8 mmole) of TMEDA to a solution of 0.99 ml (12.4 mmole) of thiophene in 50 ml of hexane and refluxing the mixture for 30 minutes. The reaction mixture was cooled to 0°C, 30 ml of THF was added and it was further cooled to -20°C. 6.9 g (22.7 mmole) of $FeCp(CO)_2I$

was added with vigorous stirring which was maintained for a further two hours while the temperature was allowed to gradually raise until room temperature was reached. After filtration through silica gel and anhydrous sodium sulphate, the solvent was removed and the residue purified using column chromatography. Four bands were distinguished on the column. The first yellow band was identified as the mono-iron complex previously synthesized by Nesmeyanov *et al*[14]. The second brown product was the starting compound $FeCp(CO)_2I$. The third red band was isolated and identified to be the iron dimer complex $[FeCp(CO)]_2$. The fourth orange compound was characterized as the diiron complex **31**, yield: 1.13 g (21%). This compound is very polar and could only be collected by using pure dichloromethane as eluent.

2.5.2 Synthesis of iron complexes 32, 33, 34 and 35

Dimetallation of 3,6-dimetylthieno[3,2-*b*]thiophene was accomplished by dissolving 0.34 g (2.0 mmole) of the ligand in 30 ml of dry diethyl ether and adding 1.4 ml (2.2 mmole) of n-butyl lithium while cooling the mixture on an ice bath. The mixture was stirred for two hours at this temperature and for a further 30 minutes at room temperature. The reaction mixture was cooled to -40°C after which 0.6 g (2.0 mmole) of $[FeCp(CO)_2I]$ was added. The reaction was stirred for 15 minutes at this temperature and for a further two hours at room temperature. Filtration through silica gel and the subsequent evaporation of the solvent *in vacuo* afforded a brown residue. Six products were isolated using column chromatography. The first organic product isolated was the starting material, DMTT, yield: 0.03 g (8%). The second yellow product was characterized as the mono iron complex **32**, yield: 0.13 g (19%). The third brown product was identified as the iron starting material $[FeCp(CO)_2I]$, yield: 0.16 g (27%). The following two orange-yellow products were found to be complexes **34** and **35**, which were isolated with yields of 0.17 g (16%) and 0.16 g (11%), respectively. The sixth orange product, complex **33**, was isolated using dichloromethane as eluent. This product was formed in a yield of 0.12 g (12%) and was characterized as the diiron complex.

2.5.3 Synthesis of tin complexes 36 and 37

Dilithiation of DMTT was effected as described in **2.3.1**. The reaction was performed using 0.674 g (4.0 mmole) of DMTT. The solution containing the dilithiated species was cooled to -

[14] A.N. Nesmeyanov, N.E. Kolobova, L.V. Goncharenko, K.N. Anisimov, *Izv. Akad. Nauk, SSSR, Ser. Khim.*, 1, **1976**, 153.

40°C and 1.594 g (8.0 mmole) of $SnMe_3Cl$ was added. The mixture was stirred at this temperature for 15 minutes and a further two hours at room temperature. The solvent was removed *in vacuo*. 100 ml of water was added to the residue and extracted with three 30 ml portions of diethyl ether. The ether extracts were combined, dried over sodium sulphate and filtered. After evaporation of the solvent, the residue was washed with hexane after which an oily residue remained. All the hexane extracts were combined, the solution was concentrated and the product left to crystallize. Complex **37** crystallized as colourless, cubic crystals from this solution, yield: 1.50 g (76%). The oily residue left in the initial flask was distilled and the mono tin complex, **36**, was afforded as a colourless oil, yield: 0.28 g (21%).

2.5.4 Synthesis of iron complex 38

Complex **37** (0.99 g; 2.0 mmole) and $[FeCp(CO)(PEt_3)I]$ (1.6 g; 4.0 mmole) were dissolved in 20 ml of DMF. The palladium catalyst $Pd(CH_3CN)_2Cl_2$ (0.025 g; 0.1 mmole) was added to the solution and the mixture was stirred for 12 hours at room temperature. Complex **38** was isolated using column chromatography (yield: 0.37 g; 24%), after collecting the green iron starting material.